CHALMERS
UNIVERSITY OF TECHNOLOGY

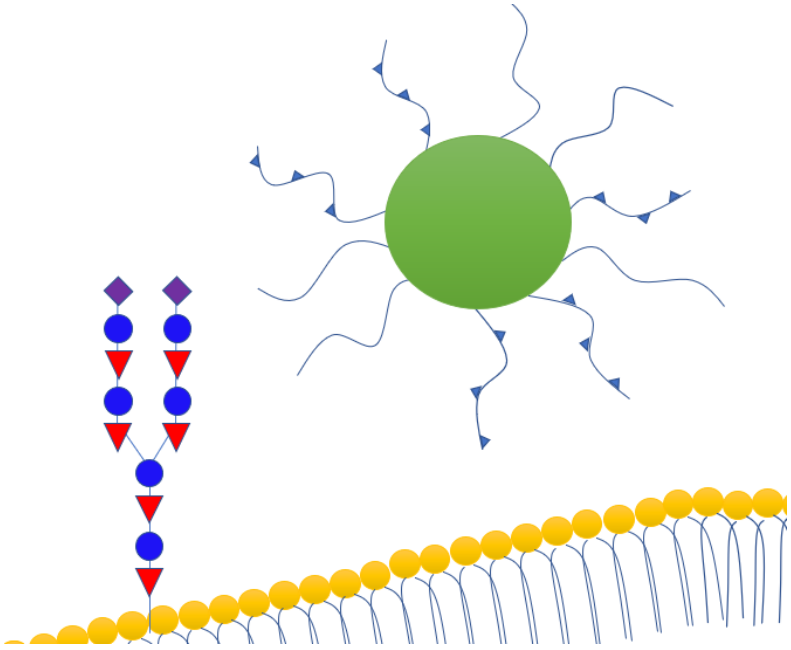

Sialic Acid Binding Nanoparticle to Inhibit Inflammation

Master's thesis in Nanotechnology

LINA PERSSON

DEPARTMENT OF BIOLOGY AND BIOLOGICAL ENGINEERING

CHALMERS UNIVERSITY OF TECHNOLOGY
Gothenburg, Sweden 2021
www.chalmers.se

Master's thesis 2021

Master thesis project aiming to inhibit proinflammatory mediators

LINA PERSSON

CHALMERS
UNIVERSITY OF TECHNOLOGY

Department of Biology and biological engineering
Chemical Biology
Stubelius Lab
Chalmers University of Technology
Gothenburg, Sweden 2021

Sialic acid binding nanoparticles to inhibit inflammation

LINA PERSSON

Supervisor: Alexandra Stubelius, Department of Chemical Biology
Examiner: Sandra Rocha, Department of Chemical Biology

Master's Thesis 2021
Department of Biology and biological engineering

STUBELIUS LAB
Chalmers University of Technology
SE-412 96 Gothenburg
Telephone +46 31 772 1000

Cover: Illustration of mimic lectin nanoparticle binding to a glycoprotein

Typeset in LaTeX
Printed by Chalmers Reproservice
Gothenburg, Sweden 2021

Sialic Acid Binding Nanoparticle Inhibits Inflammation
LINA PERSSON
Department of Nanotechnology
Chalmers University of Technology

Abstract

Inflammation is an excellent biological response that our bodies have developed to fight off foreign objects that have made their way into our bodies. In some cases, the inflammation becomes chronic as the immune system attacks healthy tissue or is unable to heal an injury. In this project the overall goal is to inhibit the inflammatory cascade using synthetic nanoparticles that mimic lectins - the natural glycobindning proteins. The particles bind sialic acid, a monosaccharide that is highly up-regulated during inflammation, and inhibits protein-protein or cell-cell interactions depending on size. The targeting moeity of the nanoparticles are phenylboronic acid (PBA) attached to branched polyethylenimine (PEI) polymers, named PBA-PEI. Isothermal titration calorimetry (ITC) and UV data show that the PBA-PEI have very high specificity and affinity towards sialic acid compared to other monosaccharides and previously published materials. Cytotoxic evaluation show that the synthesized nanoparticles are non-toxic. Furthermore, we demonstrate biological relevance of our approach in preliminary studies, where the larger nanoparticles inhibited proinflammatory activation.

Keywords: Sialic acid, Inflammation, Nanoparticles, Leukocyte recruitment, Glycoprotein.

Acknowledgements

I want to give a special thank you to Gizem Erensoy for helping me with the synthesizes in the project. Your expertise in chemistry has been of great help. I also want to thank my supervisor Alexandra Stubelius for her support and advice throughout the project. Finally, a thank you to all persons in the Stubelius lab group that have made it more fun to come to the lab. Thank you all.

Lina Persson, Gothenburg, 03 2021

Contents

List of Figures

1
Introduction

1.1 Motivation

Inflammation is something all people have encountered sometime during their life. Inflammation is an excellent biological response that our bodies have evolved to fight off foreign objects that have made their way into our body [1]. There are two types of inflammatory responses, acute and chronic, where the latter can last many years. In acute inflammation, the immune system responds to an injury or pathogen. Chronic inflammation can be the result of a disease where the immune system attacks healthy tissue. Today no treatment can reverse the damage of a chronic inflammatory disease. Treatments are dietary and lifestyle changes as well as anti-inflammatory drugs that lower the symptoms of inflammation [2].

For the inflammatory cascade to start, immune cells need to recognize that a foreign pathogen is present, and then communicate further so other cells can be recruited. This cell-to-cell or protein-to-protein signaling can be communicated via glycan modifications on proteins [3]. Glycoproteins are naturally present on all cell surfaces. As the physiological state of the cell changes, the glycome of the cell changes, presenting new glycans and glycoproteins on the cell surface. Glycoproteins consist of different sugars, also called monosaccharides [4]. One monosaccharide that is highly upregulated during inflammation is sialic acid. Sialic acid is located at the outermost end of a glycoprotein. Sialic acid therefore represents an excellent targeting candidate to stop cell-to-cell or protein-to-protein signaling and inhibit inflammatory responses.
This has previously proven to be challenging as carbohydrates are hard to target with their complex structure to obtain a high specificity. Multivalency is needed to get a strong binding. With the help of nanoparticles this can now be done [5].

1.2 Aim of this study

This project's overall goal uses synthetic nanoparticles that mimic lectins - the natural glycobinding protein to manipulate immune cell functions and inhibit the inflammatory cascade. During inflammation, leukocytes roll on the vascular endothelial cells and can then migrate into the inflamed tissue. Leukocytes roll with the help of loose binding between C-type lectins (selectins) and glycoproteins by recognizing sialic acid. Targeting sialic acid can therefore inhibit pro-inflammatory signals and leukocyte recruitment that would otherwise enhance the inflammatory cascade.

To inhibit inflammation, high affinity and specificity towards sialic acid must be achieved. The binding should be strong around pH 6, close to the pH of inflamed tissue [6]. We hypothesized that multiple phenylboronic acid (PBA) units should be attached to a branched polyethylenimine (PEI) and later nanoparticles to increase binding affinity and specificity towards sialic acid. Based on the particle size, they would be able to target different cellular functions. The smaller nanoparticles, with a core of PAMAM (polyamidoamine dendrimers) G5 and size around 5 nm were designed to inhibiting protein signaling. For the inhibition of leukocyte recruitment, a method to achieve reproducible larger poly(lactic-co-glycolic acid) (PLGA) nanoparticles with a size of 250 nm was developed. By conjugating the PEI-PBA polymers onto the particles surface at different ratios, they would be able to bind and inhibit sialic acid similar to lectins.

2

Theory

2.1 Glycans and Glycoproteins

When aiming to inhibit biological responses, glycans are excellent targets because they decorate all cells in all discovered living species. Glycans come in various sizes, shapes, charges, and other physical properties [7]. They consist of primarily ten monosaccharides: glucose (Glc), galactose (Gal), N-acetylglucosamine (GlcNAc), N-cetylgalactosamine (GalNAc), fucose (Fuc), xylose (Xyl), sialic acid (Neu5Ac), glucuronic acid (GlcA), mannose (Man) and iduronic acid (IdoA). They are linked together by glycosidic bonds, of which the orientation of the bond affects the shape of the glycan. The linkage of the glycosidic bond happens between the hydroxyl group of one monosaccharide and the other monosaccharide's anomeric carbon [3].

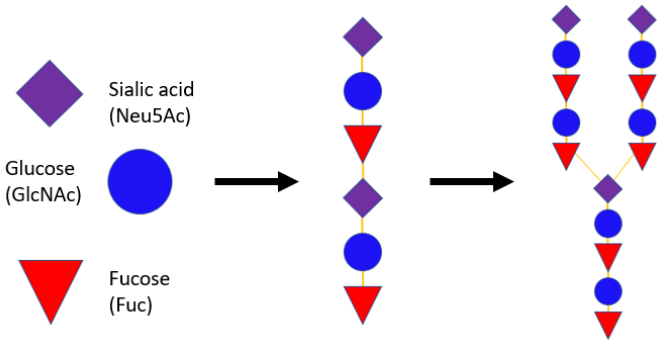

Figure 2.1: *A simplified structure of a glycan. From left to right: monosaccharides, glycans and, glycoprotein.*

As seen in the figure 2.1, the monosaccharides are the building blocks of glycans, which are part of the building blocks of glycoproteins. Due to this, the variety of possible glycoproteins are seemingly endless.

The glycome of a cell - all glycan modifications on cells - is a much more complex totality than that of the genome or proteome. Glycoproteins can mediate many functions such as cell-cell recognition, cell-matrix, or protein-protein interactions, giving them an essential role in the immune response. They can function as "pathogen-associated molecular patterns" (PAMPs) or as "danger-associated molecular patterns" (DAMPs) to enhance or suppress immune response [8]. The immune system recognizes foreign pathogen's glycomes as foreign, giving rise to different im-

mune responses [4]. Glycans are also present on antibodies, and can have different properties, being either pro-inflammatory or anti-inflammatory.

2.2 Sialic Acid

Sialic acid is one such monosaccharide with essential function for the immune system. The immune system can distinguish between a "non-self" and a "self" pattern according to the sialic acid, giving an immune response when needed [9, 10]. Sialic acid is often found at the terminal of a glycan, attached by the C-2, making it a part of many biological functions, both physical and structural. Sialic acid is negatively charged and hydrophilic. The negative charge of sialic acid works as both repulsion and attraction between cells and molecules. Sialic acid also functions as a ligand for intrinsic and extrinsic receptors [11].
The family of sialic acid is derived from the nine-carbon sugar neuraminic acid. The most common sialic acid in humans is the 5-N-acetylneuraminic acid (Neu5Ac), shown in figure 2.2.

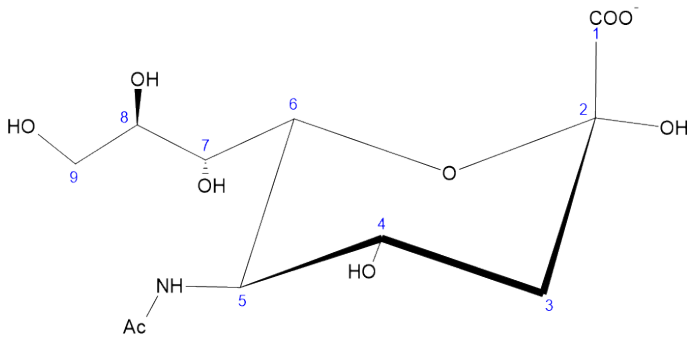

Figure 2.2: *The most common sialic acid in humans: 5-N-acetylneuraminic acid (Neu5Ac) with labeled carbon atoms.*

The carbons in sialic acid have different properties. At the C-1, a negatively charged carboxylate is located. At C-2, the anomeric center is located. The axial orientation for the carboxyl group located at C-2 is the α-anomer and is most common when sialic acid is bound to a glycan. At C-5, a different subunit is attached, which varies depending on the sialic acid. In Neu5Ac, there is an acetylated amino group at C-5. A glycerol-like side chain is at C-7 to C-9 [12].

2.3 Inflammation and the role of glycoprotein

2.3.1 Lectins

DAMPs and PAMPs can bind to pattern recognition receptors, including lectins. Lectin is a family of glycan-binding protein. They recognize the terminal groups on a glycan and can bind to it. The binding occurs in a binding pocket that is shallow but well defined. Lectins have been found in animals, plants, and microorganisms. Lectins can be found as soluble proteins, transmembrane proteins and can form oligomeric structures. An illustrative figure of a lectin is shown in figure 2.3.

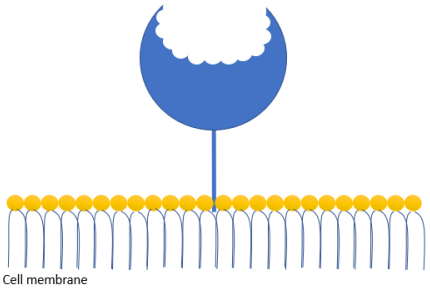

Figure 2.3: *A illustrative structure of a membrane anchored lectin.*

There are many different lectins, and they are divided into different classes depending on their amino acid sequences and biochemical properties. The lectins found in animals are the calcium-requiring (C-type) lectin. The C-type lectins includes collectins, selectins, endocytic receptors, and proteoglycans. [4, 13, 7].

Lectins can have different arrangements of carbohydrate-recognition domains (CRDs) which allows them to cross-link glycan-containing structures. This is often critical for the recognition of glycan structures and biological functions. C-type lectins recognize many different structures with high affinities. They are essential for adhesion and signaling receptors in a number of biological pathways. These pathways include homeostasis, innate immunity, and inflammatory responses. [14]

2.3.2 Selectins

C-type lectins essential for signaling receptors in many biological pathways are called selectins. Selectins can be found on the cell surface of endothelial cells, leukocytes, and platelets, called E-, L-, and P-selectins, see figure 2.4. They mediate early stages of leukocyte recruitment [14].

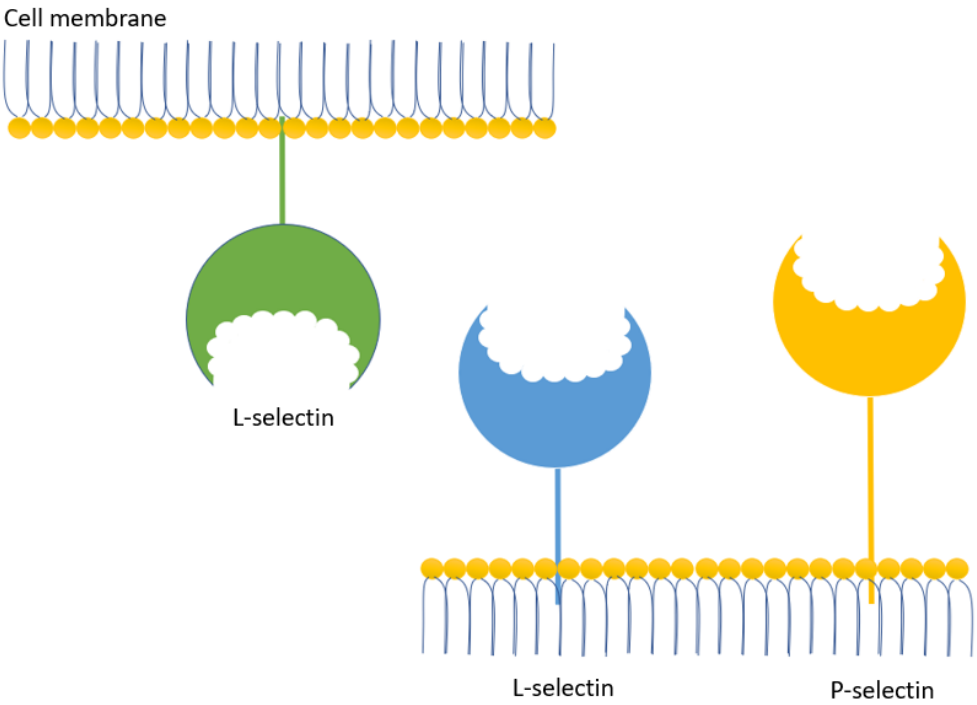

Figure 2.4: *A illustrative structure of L-, P- and E-selectins.*

P-selectins can be found on the surface of activated platelets and activated vascular endothelial cells. They are expressed on the surface due to the fusion of intracellular storage membranes with the plasma membrane. The P-selectins contribute to leukocyte recruitment, see section 2.3.3.
L-selectins are constitutively expressed on most leukocytes.
E-selectins are expressed on the cell surface of endothelial cells, and are absent under normal physiological conditions (except on the skin and bone marrow). E-selectins will be upregulated in the event of a cytokine-dependent transcriptional activation. The proinflammatory cytokines activates the endothelium to inducible E-selectins. E-selectins contribute to leukocyte recruitment in cooperation with P- and L-selectins [15, 14].

2.3.3 Leukocyte recruitment

Under normal physical conditions, the blood plasma passes close to the blood vessel wall, and the leukocytes in the middle. When the immune system reacts to a foreign object, the leukocytes are recruited to the inflamed tissue (shown in figure **??**). What kind of leukocytes that is recruited depends on the type of reaction and who/what initiated the reaction. In chronic inflammation, mainly neutrophils and macrophages are recruited [1].

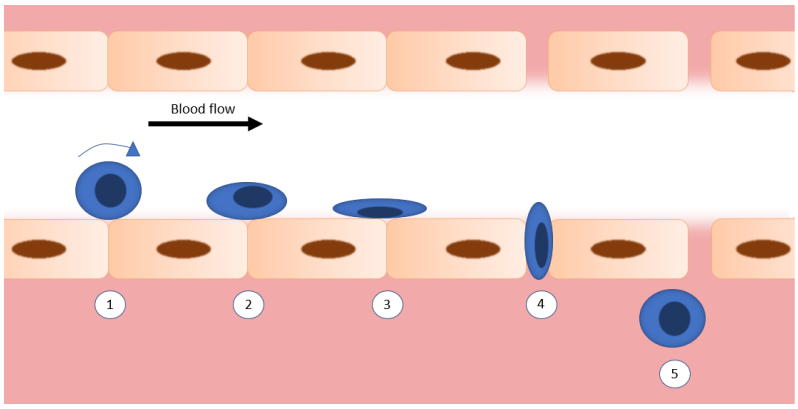

Figure 2.5: *The leukocyte recruitment process. 1. Rolling. 2. Arrest and firm adhesion. 3. Adhesion strengthening and spreading. 4. Transmigration. 5. Migration.*

The leukocyte recruitment process can be divided into five steps, seen in figure 2.5. (1) Rolling: In this step E-, and P-selectins on the endothelial cell interacts with L-selectins on the leukocyte cell surface. In the presence of an infection or injury in the body, cytokines will activate the endothelial cells, upregulating E-selectins on the endothelial cell surface. Specifically, the selectins interact with sialylated, fucosylated carbohydrate residues of sLe^X. The interactions are week, allowing the leukocyte to roll on the vascular bed. This step is reversible unless the leukocytes are activated. (2) Arrest and firm adhesion: If the leukocyte has been activated, they bind tightly to ligands on the endothelial cell surface. These ligands are called adhesion molecule 1 and 2 or ICAM-1 and ICAM-2, respectively. The tight biding allows for the rolling to stop, and a firm adhesion forms. (3) Adhesion strengthening and spreading: When a stable arrest is formed, the leukocytes flatten on the endothelial surface, which also can help to strengthen the binding between the adhesion molecules and ligands. The spreading happens most likely to avoid collision with circulating blood cells and to reduce the shear stress from blood flow. The leukocytes will begin to crawl, which can happen both against and with blood flow, to an endothelial border. The crawling is mediated by interactions between ICAM-1 on the endothelial cell and the integrin Mac-1 on the leukocyte. (4) Transmigration: At the endothelial cell border, the leukocytes will cross between endothelial cells preferably where there are less collagen and laminin densities which allows for gaps in the ECM structure. In rare cases, the leukocytes will cross the endothelial cell body. (5) Migration: The leukocyte migrates into the inflamed tissue [16, 17, 18].

2.4 Material choice

2.4.1 Phenylboronic Acid - PBA

Carbohydrates and monosaccharides can interact with phenylboronic acids (PBAs), which are known to bind diol groups on carbohydrates and sialic acid. Due to PBA selactivity torwards sialic acid it can work as a synthetic mimic of lectin. The resulting boronic ester is one of the strongest reversible single-pair functional groups in an aqueous environment [19]. The formation of the strong functional groups makes boronic acid-containing constructs an excellent tool for targeting glycoproteins [20]. There are two possible diols on sialic acid that PBA can bind to, the α-hydroxyacid or the glycerol-like chain (see figure 2.6). [21, 22]

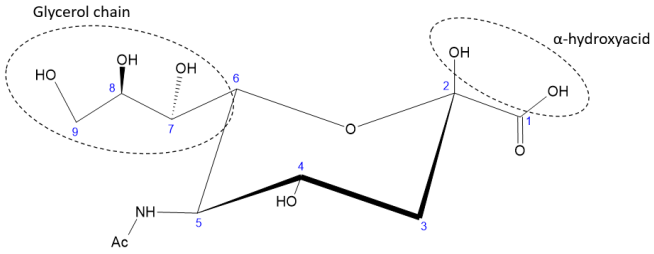

Figure 2.6: *Possible binding sites for PBA to sialic acid.*

The hydroxyl group on PBA reacts to one of the two binding sites on sialic acid, seen in figure 2.6. The α-hydroxyacid grup on sialic acid is bound to the glycoproteins, meaning PBA will bind exclusively to the glycerol chain, see figure 2.7 [21].

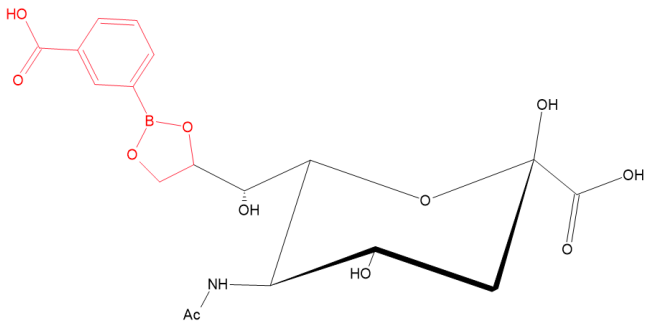

Figure 2.7: *PBA bound to sialic acid.*

It has been reported that PBA selectivity recognizes sialic acid with a high K value [23]. PBA can also recognize other common sugars such as glucose and fructose. Sialic acid and PBA complexes are, however, stable when the pH value is lower than its pK_a value (pK_a is a value associated with the acid dissociation constant K_a and is defined as $pK_a = -log_{10}K_a$) [24, 25]. The PBA targeting moiety is shown in figure 2.8.

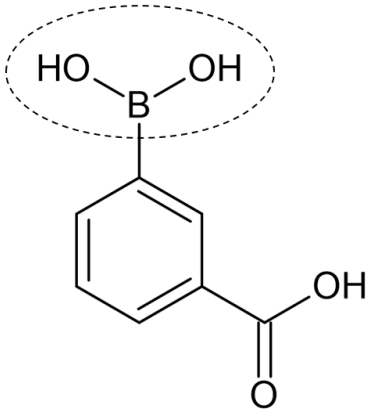

Figure 2.8: *3-Carboxyphenylboronic acid that is used in this project with targeting moiety (hydroxyl group) for sialic acid.*

2.4.2 Polyethylenimine - PEI

Polyethylenimine (PEI) is a polymer with repeating units as seen in figure 2.9.

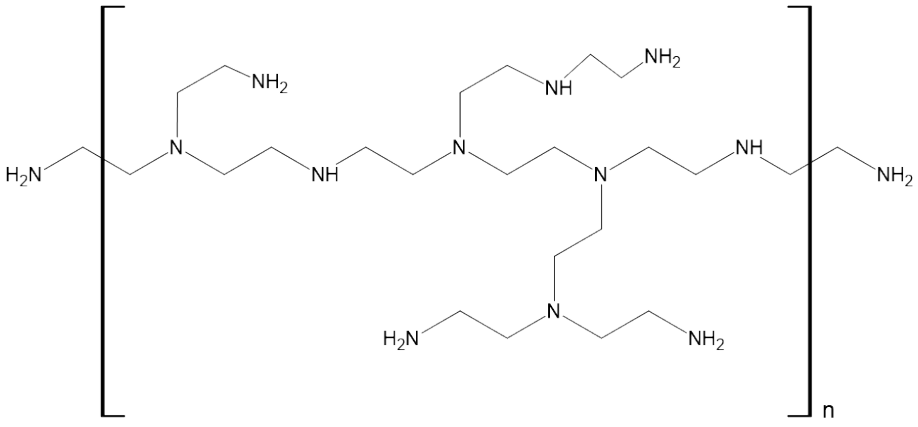

Figure 2.9: *Branced Polyethylenimine (PEI).*

The polymer has a high charge density in physiological media [26]. In this project, the high charge density from the polymer is hypothesized to interact with the negatively charged sialic acid. Furthermore, one of the amino groups in PEI will be conjugated with a PBA as seen in figure 2.10. PBA conjugated to PEI is hypothesized to further increase binding and specificity.

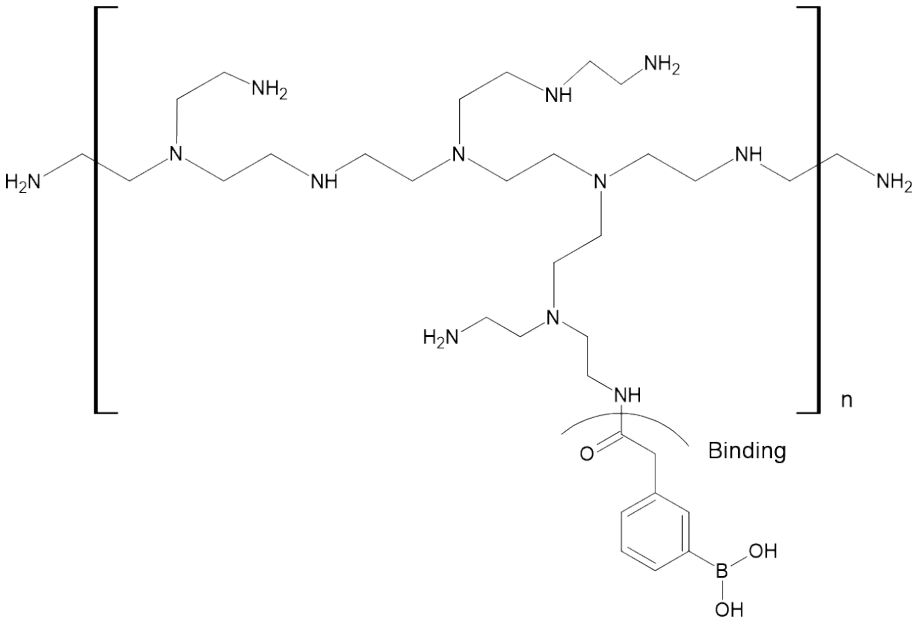

Figure 2.10: *PBA bound to PEI.*

Additional amino groups will remain free after PBA has been conjugated to PEI. The unreacted amino groups will act as additional binding sites to the hydroxyl groups on sialic acid via electrostatic interactions. To understand if the unreacted amino groups will influence the binding with sialic acid two different length will be tested.

2.4.3 Polyamidoamine - PAMAM

Polyamidoamine (PAMAM) is a dendrimer that consist of an ethylenediamine core and repeating branches of amidoamine. PAMAM comes in different generations with a varying number of branches. The dendrimers have a well-controlled structure and are therefore popular to use as carriers in nanomedicine. PAMAM has a branched structure, one unit of the most outer branches is presented in figure 2.11.

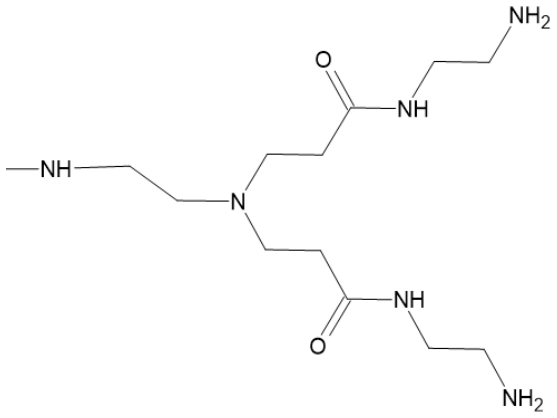

Figure 2.11: *Outer branch of PAMAM G5. A primary amine group is located at each branch and a trertairy amine group at each branching point.*

PAMAM G5 has 4548 atoms with 128 primary nitrogens and 126 tertiary nitrogens. The primary amine group is located at each branch, and the tertiary amine group at each branching point. The PAMAM size is influenced by pH. The electrostatic repulsion between the amino groups at neutral to low pH will cause the branches to stretch out, increasing the size [27]. PAMAM have a high toxicity both *in vitro* and *in vivo* due to the highly positive surface charge. To achieve better biocompatibility, it is therefore important to tune the surface charge of the dendrimer [28].

2.4.4 Poly(lactic-co-glycolic acid) - PLGA

Poly(lactic-co-glycolic acid) (PLGA) particles are commonly used in biological applications. PLGA particles have been tested for biocompatibility, and in low concentrations, there have been no reports of accumulation in the body. PLGA is a co-polymer of D,L-lactic acid with glycolic acid. PLGA is soluble in many solvents and can easily be synthesized into particles. [29].
There are several different approaches to synthesizing PLGA particles. One of the most commonly used is an emulsification-solvent evaporation technique. This involves oil in water phase or, in the case of a double emulsion, a water/oil/water phase. Another technique is using an electrospray system to synthesize the PLGA. Both approaches are commonly used to encapsulat drugs [30, 31].
In this project, PLGA nanoparticles was prepared using nano-precipitation [32]. Nano-precipitation is a method were a solvent phase (polymer) is dropped in a non-solvent phase (surfactant), and the solution is stirred with a magnetic stirrer. The

two solution are miscible with each other and hydrophobic interactions will drive the reaction [33]. In this project, a PLGA core will be surrounded by a polyethylene glycol (PEG) surfactant. As a surfactant, PEG is a water-miscible to provide an interface between the core PLGA in the and the outer water phase. PEG is non-toxic and has been used to shield nanoparticles from immune recognition [34, 35]. For targeting, PEG is conjugated with PBA-PEI and these targeting moieties will be incorporated at different rations of nonconjugated PEG to PBA-PEI-PEG as surfactants. A schematic figure of the nanoparticle is shown in figure 2.12.

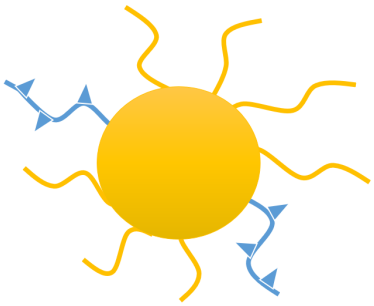

Figure 2.12: *PLGA nanoparticle with PEG (yellow) and conjugated PBA-PEI chains (blue).*

2.5 Other approaches to inhibit inflammation

Glycan-targeting research approaches have expanded in the last few years, focusing on different receptors involved in pathogen recognition and activation of macrophages. Other research groups have focused on identifying pathways for pro-inflammatory signals and stop these [36]. The wide approaches to interpret the glycome of cells are all possible advances to stop inflammatory responses.

Inorganic nanoparticles have been studied as drug carriers to inhibit inflammation. Gold nanoparticles have been widely researched due to its biocompatibility, plasmon resonance properties and, drug loading abilities. Due to well-defined structural properties the previous mentioned qualities of the nanoparticle can be fine-tuned and allow for surface modifications [37].

Anti-inflammatory drugs is commonly used to suppress and treat inflammation. The drawback with the drugs is that they often give side effects. The side effects can vary in gravity and cause heart attack, stroke and liver problems **??**.

Lifestyle habits such as exercise, diet and stress have also been linked to inflammation. Unhealthy lifestyle choices can cause muscle stress, overexpressed inflammatory cytokine and, tissue damage [38, 39]. Inflammation caused by unhealthy lifestyle habits can often be avoided with a balanced diet and exercise.

3

Methods and Material

3.1 PBA-PEI synthesis

The protocol for PBA-PEI was developed by Gizem Erensoy. NMR data to confirm the conjugation of PBA to PEI is given in appendix B.

3.1.1 PBA-PEI polymer

The PBA-PEI polymer was synthesized as follows: 200 mg of 3-Carboxybenzeneboronic acid pinacol ester (PBA) (purchased from Alfa Aesar, mw 165.95 g/mol) was dissolved in 20 ml methanol $\geq$ 99.9% (purchased from Fisher Chemical) under nitrogen gas. The solution was stirred in room temperate under nitrogen gas. 560 mg of 1-(3-Dimethylaminopropyl)-3-ethylcarbodiimide hydrochloride, 98+% (EDC) (purchased from Alfa Aesar, mw 155.24 g/mol), and 200 mg of N-hydroxysuccinimide (NHS) (purchased from Thermo Scientific) was added into the solution, then stirred for four hours under nitrogen gas.
For PBA-PEI_{800}: 320 mg of Polyethylenimine, branched (PEI) (purchased from Sigma-Aldrich, mw 800 g/mol) was added to the solution.
For PBA-PEI_{2000}: 800 mg of PEI Polyethylenimine, branched (PEI) (purchased from Sigma-Aldrich, mw 2000 g/mol) was added to the solution.
PEI was added to the solution and stirred for 24 hours under nitrogen gas. On ice, Diethyl Ether (Anhydrous, Extra Dry, for Synthesis, Stabilised with Pyrogal. Purchased from Fisher) was added to the PBA-PEI solution. The white compound was collected from the mixture and dried in a freeze dryer. NMR data for the PBA-PEI can be found in appendix...

3.1.2 PBA-PEI conjugation to mPEG

1.00 g of Poly(ethylene glycol) methyl ether (mPEG) (purchased from Sigma-Aldrich, mw 20000 g/mol) and 22.40 mg 4-nitrophenyl-chloroformate, 97% (4-NPC) (purchased from Acros Organics, mw 201.57 g/mol) was added with 6.79 mg 4-dimethylaminopyridine (DMAP) (purchased from Sigma-Aldrich, mw 122.17 g/mol) and flushed with nitrogen gas for 10 minutes. Under stirring and room temperature, Dichloromethane, anhydrous, 99.7+ % (purchased from Alfa Aesar) was added dropwise to the solution until the solution was clear, the solution was stirred for 24 h.
A solution of the PBA-PEI polymer in 10 % (v/v) Sodium hydrogen carbonate ($NaHCO_3$) in milli-Q was made and adjusted to pH to 8 with HCl.

The synthesized mPEG-4-NPC was solubilized in approximately 2 ml Methyl Sulfoxide, 99.7+% (DMSO) (purchased from Acros Organics), sonicate mixture. mPEG-4-NPC was mixed in DMSO with PBA-PEI. DMSO should be 10-20 % of the total volume in the solution. The mixture was vortex. The reaction vessel was covered with foil and incubated overnight at room temperature while rotating. Dialyze was done to the solution with a DMSO compatible membrane for 24h to remove DMSO and unreacted mPEG-4NPC. The mixture was then lyophilized.

3.2 Binding specificity

3.2.1 UV-vis

A competitive assay was done with Alizarin Red S (ARS) (purchased from Fisher Chemical, mw 342.253 g/mol), 3-Carboxybenzeneboronic acid pinacol ester (PBA) (purchased from Alfa Aesar, mw 165.95 g/mol), and D-fructose (purchased from Alfa Aesar, mw: 180.16 g/mol). Quartz cuvettes were used. The UV spectra were measured in a the Varian Cary® 50 UV-Vis Spectrophotometer. ARS was mixed in PBS to $10^{-}4$M solution, PBA was mixed in PBS to $10^{-}3$M solution, and fructose was mixed in PBS to 0.1M solution. All different solutions (ARS, PBA, and fructose) were mixed as a 1:1 or a 1:1:1 solution. PBS was used as a baseline for the absorption spectra. The following measurements were done: ARS alone, PBA with ARS and, PBA with ARS and fructose. The pH was adjusted to 7.4 and 6.0 with 0.1 mM $NaHCO_3$ solution and 0.1 mM HCl solution.

3.2.2 Isothermal Titration Calorimetry - ITC

Malvern MicroCal iTC200 was used to measure the binding constant (K_d) between PBA-PEI and the monosaccharides sialic acid, fructose, and glucose at different pH. N-Acetylneuraminic acid (sialic acid) (purchased from Acros Organics, mw 309.27 g/mol), D-fructose (purchased from Alfa Aesar, mw: 180.16 g/mol), and D-glucose (purchased from Alfa Aesar, mw: 180.16 g/mol) was mixed to an 80 mM solution in Milli-Q water. The PBA-PEI polymer was dissolved in Milli-Q water to obtain molarity of 2 mM. When calculating the molarity for PBA-PEI, the molecular weight was for PBA (mw 443.82 g/mol). The reference cell in the ITC was filled with Milli-Q water.
In total twenty titrations were done at 25°C. The first was a 1 μL titration that lasted 2 seconds. After the first, nineteen, 2 μL, titrations each lasting for 4 seconds was done. For fructose and sialic acid, the time between titrations was set to 180 seconds. For glucose the time between titrations was 360 seconds.

3.3 Synthesize of nanoparticles

3.3.1 PLGA Nanoparticles

Two different PLGA particles were synthesized. One with one PBA-PEI chain every ten PEG, and one with one PBA-PEI chain every fifty PEG. The PLGA particles will be referred to as PLGA 1:10 and PLGA 1:50, respectively. On mPEG, a PBA-PEI_{2000} was conjugated, see section 3.1.2. The method development for the PLGA nanoparticles is described in A.1.

For PLGA 1:10: 50 mg of mPEG-PBA-PEI_{2000} (mw 22443.82 g/mol) and 561.1 mg Polyethylene glycol (PEG) (purchased from Sigma-Aldrich, mw 20 000 g/mol) was dissolved in 61.1 mL milli-Q water for a 1 % solution.
For PLGA 1:50: 10 mg of PEG-PBA-PEI_{2000} (mw 22443.82 g/mol) and 561.1 mg PEG (MW 20 000 g/mol) was dissolved in 57.1 mL milli-Q water for a 1 % solution. PLGA (poly(lactic-co-glycolic acid)) (purchased from Sigma-Aldrich, mw 7000-17000 g/mol) was dissolved in acetone to a concentration of 17 mg/mL. During stirring, 2 mL PLGA per 100 mL 1 % PEG solution was added dropwise to the water solution. The solution was stirred at 500 rpm overnight in room temperature.

3.3.2 PAMAM

The PAMAM G5 particles (purchased from Sigma-Aldrich) with conjugated PBA were synthesized by Gizem Erensoy. The protocol for the PAMAM-PBA synthesis is given in Appendix B.

3.4 Nanoparticle characterization

3.4.1 DLS

The size and zeta potential of conjugated nanoparticles PLGA and PAMAM were measured using Zetasizer Nano ZS from Malvern Panalytical. For size measurement, disposable UV Micro cuvettes (purchased from Sigma-Aldrich) were used and for zeta potential, Folded Capillary Zeta Cell DTS1070 (purchased from Malvern Panalytical) was used. A 30 μM solution of PAMAM was mixed in Milli-Q water. The PLGA particles were diluted 1:10 directly after tangential flow. 600 μL was used in the size measurement. The size measurements were done in 3 repeats with 10 measurements of each repeat. For the zeta potential, 800 μL was added to the Folded Capillary Zeta Cell. The zeta potential was done in 10 repeats with 100 measurements for each repeat.

3.5 Cell studies

3.5.1 Cytotoxicity

For the cell cytotoxicity, the cell line L-929 fibroblast (CCL1, ATCC) was used. DMEM (purchased from Thermo Fisher Scientific) with 10 % Fetal Bovine Serum (purchased from Sigma-Aldrich) and 1 % Sodium Pyruvate (100mM) (purchased from Life Technologies) as complete media was used to culture the cells. The cells were treated with PLGA 1:10, PLGA 1:50, and PAMAM at six different concentrations. The concentrations were 2.5 μg/mL, 10 μg/mL, 25 μg/mL, 50 μg/mL, 75 μg/mL, and 100 μg/mL. The nanoparticles were dissolved in Dulbecco's Phosphate-Buffered Saline DPBS (1X) (+ Ca,+ Mg) (Corning). The toxicity was measured after 24 h and after 48 h. The live cell and treated cell were done in triplicates. The incubation is done at 37°C and 5% CO_2.
In a 96-well plate 20 000 cells in 100 μL was seeded per well. After 24 h incubation, the cells were treated additional 80 μL of complete DMEM and 20 μL nanoparticle solution. After an additional 24 h alternative, 48 h incubation, 10 μL of resazurin reagent was added to each well and incubated for 3 h until media had turned pink. Detection of fluorescence was done using a 560 excitation and 590 emission filter.
For negative control, live cells were used.

3.5.2 Transwell Migration Assay

In the migration assay, HL60 neutrophils were used. The plate used was Corning™ Transwell™ Multiple Well Plate with Permeable Polycarbonate Membrane Inserts (Fisher Scientific). The cells were cultured in RPMI Medium 1640 (1X) (Thermo Fisher Scientific). To complete the media, 10 % Fetal Bovine Serum (Sigma-Aldrich) and 1 % Sodium Pyruvate (100mM) (Life Technologies) was added. To differentiate the HL60, 1.3 % Dimethyl Sulfoxide (DMSO) (Fisher Chemical) was added during culturing.
The plate has six wells that is divided with a top well and a bottom well, seen in figure 3.1.

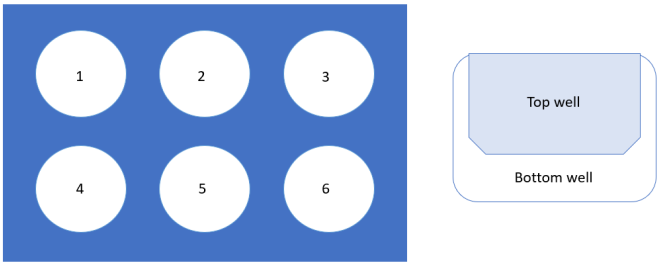

Figure 3.1: *Layout of the plate. In the wells following was added: 1. Top: HL60, bottom: Media. 2. Top: HL60, bottom: Media + LPS. 3. Top: HL60 + control PLGA 1:10, bottom: Media + LPS. 4. Top: HL60 + PLGA 1:10, bottom: Media + LPS. 5. Top: HL60 + PLGA 1:50, bottom: Media + LPS. 6. Top: HL60 + PAMAM, bottom: Media + LPS.*

Briefly, the the HL60 cells were activated, loaded onto the top well and let to migrate towards the bottom well for four hours. The cells migrated towards Lipopolysaccharide (LPS) after being treated with the particles. The wells were treated as following: 1. Top: HL60, bottom: Media. 2. Top: HL60, bottom: Media + LPS. 3. Top: HL60 + control PLGA 1:10, bottom: Media + LPS. 4. Top: HL60 + PLGA 1:10, bottom: Media + LPS. 5. Top: HL60 + PLGA 1:50, bottom: Media + LPS. 6. Top: HL60 + PAMAM, bottom: Media + LPS.
Cells were set to 500 000 per mL per and activated with Phorbol myristate acetate (PMA) (Sigma-Aldrich) for 60 minutes in a falcon tube in the incubator at 37°C, the final concentration of PMA was 50nM. The cells were washed two times with complete media. 500 000 cells in 1 ml were plated in each top well. The cells were treated with PLGA 1:10, PLGA 1:50, PAMAM for a final concentration of 100 μg/mL. As positive control, HL60 migrated towards LPS. As negative control we used HL60 migrating media and, PLGA without PBA-PEI. In all bottom wells, 2 ml of media was added. In five of the bottom wells, 100 ng/mL LPS (Purchased from Sigma-Aldrich) was added to stimulate migration.
After a 4-hour incubation, cells were counted from both the top and the bottom well using a Thermo Fisher Scientific Invitrogen Countess 3. All cells were counted twice.

3.6 Statistical method

A one-way ANOVA was used for the statistical analysis of the cytotoxicity studies. Each concentration of treated cells was compared with live cells, set to 1. One-way ANOVA calculations were performed in MATLAB.

4

Results and Discussion

4.1 Binding Specificity

The binding specificity of PBA, PBA-PEI_{800} and PBA-PEI_{2000} was evaluated using two different methods, UV-vis and ITC. UV-vis is a fast technique and can show the difference in absorption spectra of the PBA when bound and unbound to a dye. ITC is a highly sensitive technique that eliminates the need for labels. Another advantage of ITC is the small volumes required for measurements. ITC gives the binding affinity between PBA-PEI and monosaccharides.

4.1.1 UV-vis

A competitive binding assay was performed with UV-vis to evaluate the binding specificity of PBA to monosaccharides. PBA binds to diols, OH groups, present on monosaccharides and the dye Alizarin red S (ARS). Comparing the absorption spectra for PBA with the absorption spectra of ARS and fructose, the selectivity to monosaccharides could be determined. We further evaluated the binding specificity to monosaccharides at both pH 6 and pH 7.4 (figure 4.1 and 4.2). Physiological pH under normal conditions is around 7.4, while during inflammation, the pH value is around 6.

To confirm binding of PBA to ARS, the absorption maximum was analysed. Shifting of maximum indicated that PBA had bound to ARS. At pH 6 the absorption maximum for ARS was 507 nm (figure 4.1). The absorption maximum had shifted to 464 nm when PBA was mixed with ARS. To validate that ARS had bound to PBA instead of fructose, the absorption maximum should be the same as for PBA and ARS. PBA with both fructose and ARS had an absorption maximum of 481 nm. This suggested that PBA had bound to both ARS and fructose. If all PBA had bound to ARS there should be no difference in the absorption spectra between ARS with PBA and - PBA with fructose and ARS. Therefore, these findings demonstrated that at pH 6, PBA bounds to fructose with a lower affinity than to ARS.

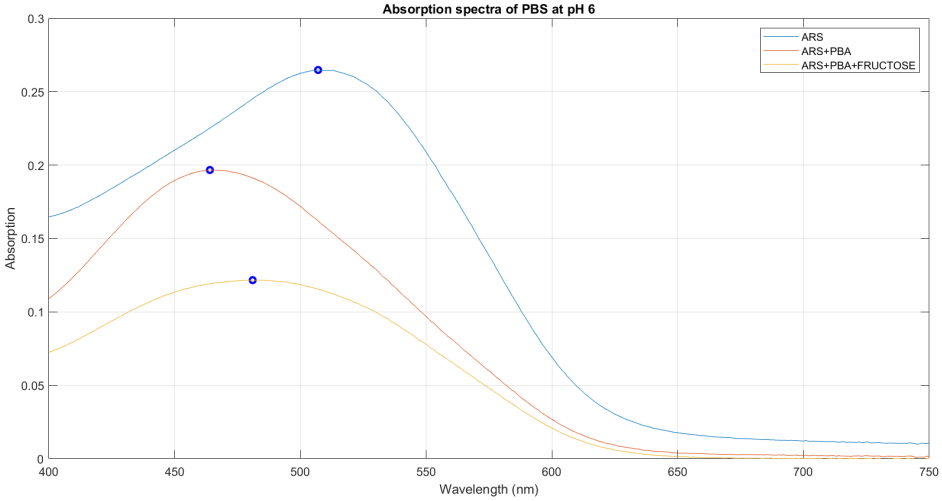

Figure 4.1: *Spectral data of PBA and ARS at pH 6. Absorption max for ARS is 507 nm, ARS+PBA 464 nm, ARS+PBA+FRUC 481 nm. PBA binds to both ARS and fructose and have therefor no selectivity for fructose at pH 6.*

The maximum at pH 7.4 was 511 nm for ARS (figure 4.2). To confirm binding between ARS and PBA the absorption maximum should have shifted from 511 nm. ARS and PBA had an absorption maximum at 480 nm, indicating that PBA had bound to ARS. To validate that PBA favoured binding to fructose instead of ARS the absorption maximum should be close to 511 nm, as it was for only ARS. PBA with ARS and fructose had an absorption maximum at 512 nm, demonstrating that PBA had bound to only fructose. This was a strong indication that PBA selectively had bound to fructose at pH 7.4 and that PBA had a pH-dependent binding of ARS.

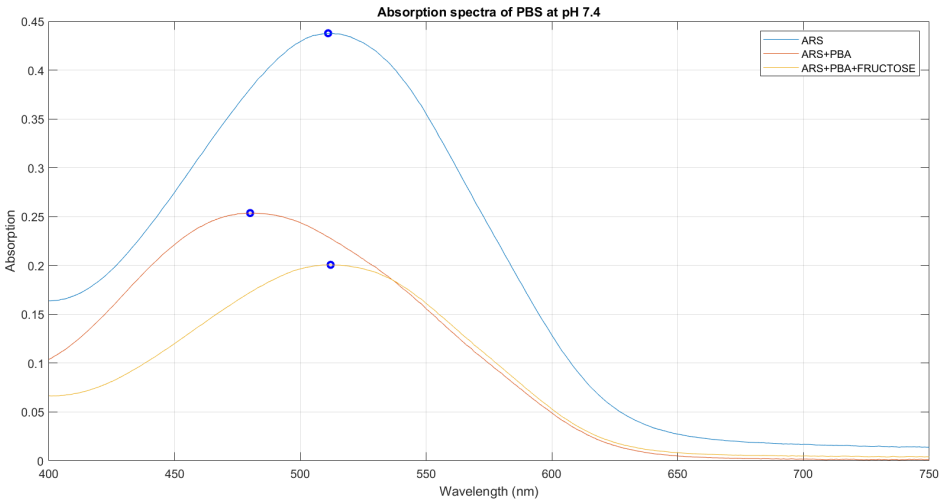

Figure 4.2: *Spectral data of PBA and ARS at pH 7.4. Absorption max for ARS is 511 nm, ARS+PBA 480 nm, ARS+PBA+FRUC 512 nm. PBA binds fructose stronger at pH 7.4 than at pH 6.*

The pK_a further influenced the binding constant, and from published material [19], it has been shown that the binding constant between PBA and fructose becomes higher as pH increase. The pK_a of fructose is around 12 at 18°C [40]. As the pK_a of fructose is higher than the pH tested, it was probable that the complexes formed between PBA and fructose were not stable. This information could further explain the results in figure 4.1 and 4.2. If the complex formed had higher pH stability, the probability for ARS to bind to PBA should have been lower at higher pH.

Due to the large amount of material needed for this UV-based assay (necessitating very high molarity, 0.1 M), the binding specificity with sialic acid and PBA was not carried out. Due to the pK_a for sialic acid being between 2.2-3.0 [41], it would probably have had formed a more stable complex with the PBA at pH 6 than for fructose. This suggested a strong selective binding of PBA to sialic acid than that for fructose.

4.1.2 Isothermal Titration Calometry - ITC

To confirm the UV-based binding affinities and get more detailed information about the binding reaction, ITC was used. With this assay's ability to determine binding affinity, it was seen as the most valid method to use in this project. The method of ITC is to load a sample cell with X and a syringe with Y. The ITC will then measure the heat loss or gain when binding between the two occurs. Binding affinity has a relation with pH and pK_a, as discussed above. The physiological pH is around 7.4, and when inflammation occurs, the tissue's pH is about 6. Due to this project's focus on inflammation, most ITC measurements were therefore performed at this lower pH of 6. The slope of the obtained curve will result in a calculation of the binding affinity.

For this assay, we tested the two PBA-PEI polymers to evaluate their specificity and binding affinities. To validate that PBA-PEI had a higher specificity to sialic acid than other monosaccharides, the binding affinity for PBA-PEI to sialic acid should have had the highest value. At pH 6, PBA-PEI_{800} was tested to fructose and sialic acid (figure 4.3). We confirmed from ITC measurements that fructose to PBA-PEI_{800} had a binding affinity of 89 M^{-1} and, for sialic acid to PBA-PEI_{800} the binding affinity was 6140 M^{-1}. The high difference between the binding affinities could be a result of different pK_a as well as specificity to sialic acid, as the binding affinity was 69 times higher for PBA-PEI_{800} to sialic acid than for PBA-PEI_{800} to fructose.

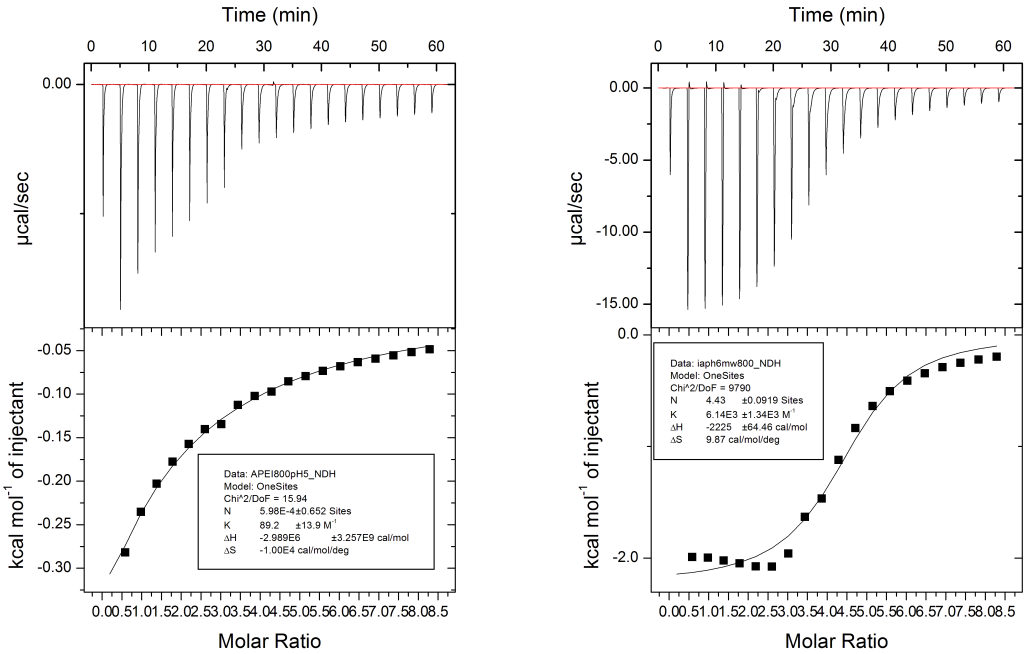

Figure 4.3: *ITC data for two different monosaccharides to PBA-PEI_{800} at pH 6. Left: Fructose to PBA-PEI_{800}. Right: sialic acid to PBA-PEI_{800}. The binding affinity is 89 M^{-1} and 6140 M^{-1} respectively.*

To evaluate how the pH could have influenced the binding affinity, ITC was executed with PBA-PEI$_{2000}$ to sialic acid at pH 5 and pH 6, the results are shown in figure 4.4.

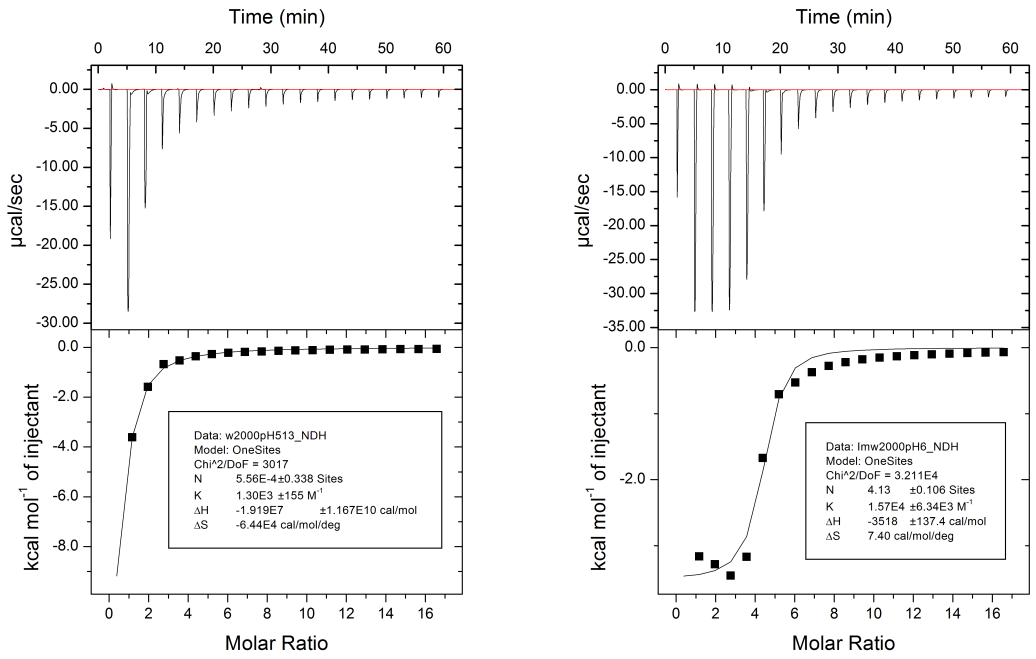

Figure 4.4: *ITC data for sialic acid to PBA-PEI$_{2000}$ at different pH. Left: pH 5. Right: pH 6.*

The binding affinity was 15700 M^{-1} at pH 6 and 13000 M^{-1} at pH 5. This showed a trend of higher binding affinity at higher pH. However, as seen in the left figure 4.4 the ITC spectra were not optimal - the curvature of the titration curve was too steep. The slope of the curve indicated a kinetic that was too fast for the measurement to be accurate. This could be due to a high concentration of sialic acid in the syringe, leading to the biding sites on PBA-PEI$_{2000}$ filled up too quickly, which led to a steeper curve. The binding sites for an ITC measurement should not be used up immediately as it will give a wrong value for the binding affinity when comparing the results.

Comparing the binding affinity at pH 6 between sialic acid to PBA-PEI$_{2000}$, and sialic acid to PBA-PEI$_{800}$ (right figure 4.3) the binding affinity for PBA-PEI$_{2000}$ was 2.5 folds higher. From these findings, the most promising candidate to use for targeting sialic acid in inflammation and continue with PLGA nanoparticle synthesis was PBA-PEI$_{2000}$.

To determine the selectivity of PBA-PEI$_{2000}$ to sialic acid at pH 6, ITC was performed with fructose and glucose. These findings are presented in figure 4.5.

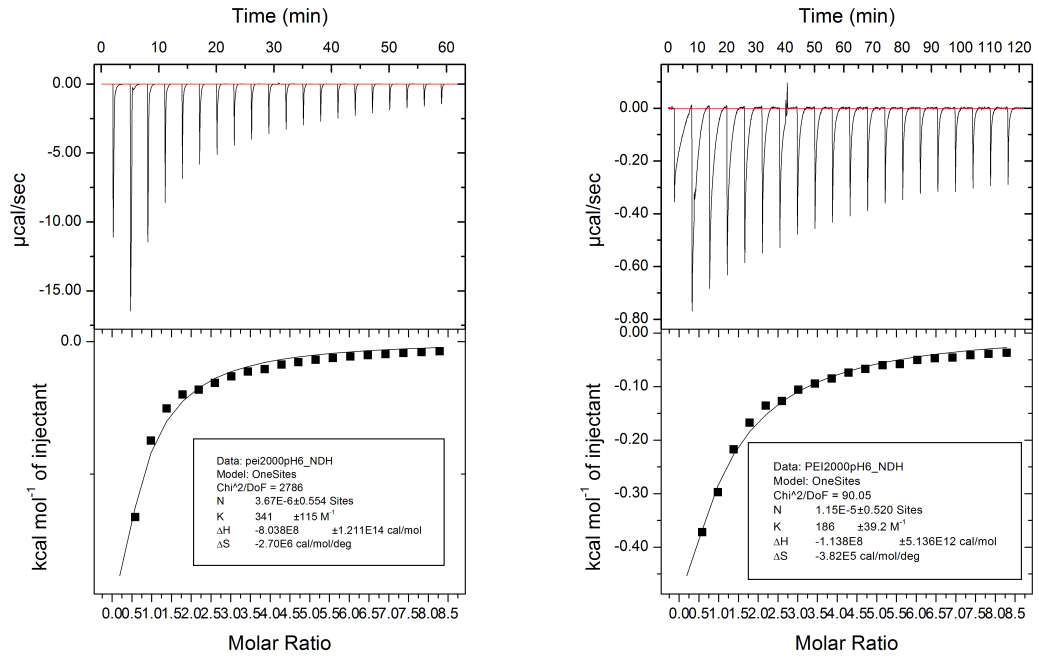

Figure 4.5: *ITC data for fructose and glucose to PBA-PEI$_{2000}$ at pH 6. Left: Fructose to PBA-PEI$_{2000}$. Right: Glucose to PBA-PEI$_{2000}$.*

The findings showed that when comparing fructose to glucose that PBA-PEI$_{2000}$ bound fructose with a higher affinity than glucose (341 M^{-1} and 186 M^{-1} respectively). Additionally, the time between injections had to be increased for the glucose sample. The glucose sample did not equilibrate as fast as measuring fructose and sialic acid, which indicated a slower binding kinetic. At pH 6 the binding affinity for sialic acid was 15700 M^{-1} (figure 4.4). That was 46 times higher than the binding affinity for fructose at pH 6 and 84 times higher than the binding affinity for glucose at pH 6. This demonstrated not only a strong binding but also a high selectivity of PBA-PEI$_{2000}$ to sialic acid.

Previously published articles about binding affinities with benzoboroxole-based receptors to sialic acid ([21]), reported highest binding affinity of 234.3 M^{-1} at pH 5.5. The highest binding affinity from the ITC mesurments was 15700 M^{-1} at pH 6 for PBA-PEI. As discussed above, the pK_a would likely have influenced the binding affinity further. The binding affinity between PBA-PEI and sialic acid would likely increase at pH 5.5. From this we could conclude that our synthesis of a target molecule, PBA-PEI, for sialic acid had been successful.

4.2 Nanoparticle Characterization

The size characterization would reveal if the synthesis of the nanoparticles were successful. Charge characterization could indicate potential cytotoxicity. Furthermore, the particle surface charge at different pH could give an understanding of how

the nanoparticles function and bind sialic acid at different pH. The nanoparticle's charge and hydrodynamic size were characterized with DLS. To evaluate if pH influenced the nanoparticles' size and charge, the measurement was performed at pH 5, 6, and 7.4. It was hypothesized that larger PLGA-PBA nanoparticles would inhibit leukocyte migration, and smaller nanoparticles, PAMAM-PBA, would inhibit protein-protein interactions.

4.2.1 Size

From DLS size measurements in figure 4.6, it was clear that pH did not influence the size of PLGA 1:10 nanoparticles. The Z-average size (intensity weighted mean hydrodynamic size) of PLGA 1:10 spanned between 252.2 nm to 253.0 nm. To further enhance and validate the results, the DLS size measurements could have been done over time. A second measurement was performed after three days during the method development for PLGA nanoparticles (see Appendix 1). The result showed that the non-conjugated PLGA particles were stable as their size remained unchanged after the three days.

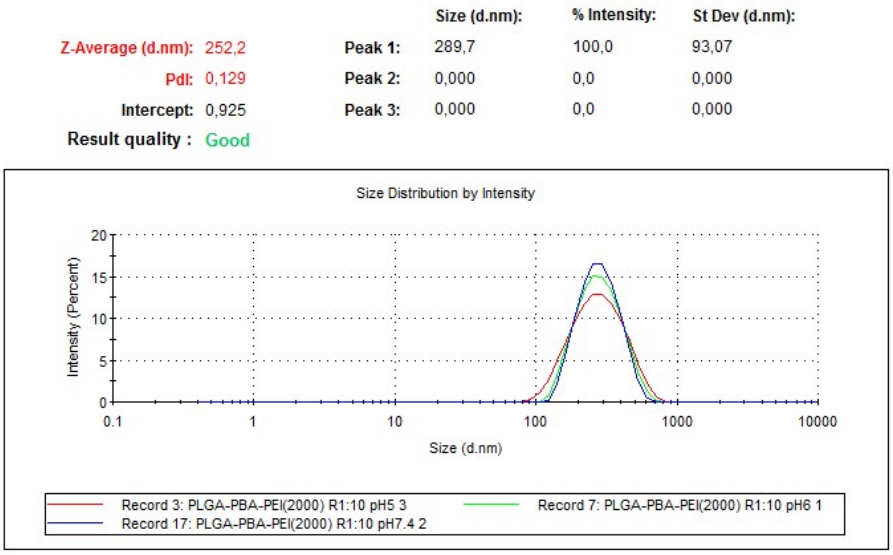

Figure 4.6: *Size for PLGA 1:10 measured with DLS at different pH values. Red line - pH 5. Green line - pH 6. Blue line - pH 7.4. The pH has no effect on the size of the nanoparticles which is around 252 nm in diameter.*

Interestingly, the PLGA 1:50 nanoparticles demonstrated a pH-dependency, as the Z-average size ranged from 276.6 nm to 320.6 nm (figure 4.7). For pH 5 and pH 7.4, the size was close to each other, 283.1 nm and 276.6 nm, respectively. For pH 6 the average size was 320.6 nm. This discrepancy may indicate a conformational change in the surfactant configuration or there was a measurement error. If pH influenced PLGA 1:50, the size difference between pH 5 and pH 7.4 should have been significantly different. The results at pH 6 instead indicated potential contamination in contact with the solution. The contamination was probably due to handling error when the pH was adjusted, as all PLGA 1:50 solutions were prepared from the same

batch. Due to material shortage, a second evaluation could not be performed that validated these results.

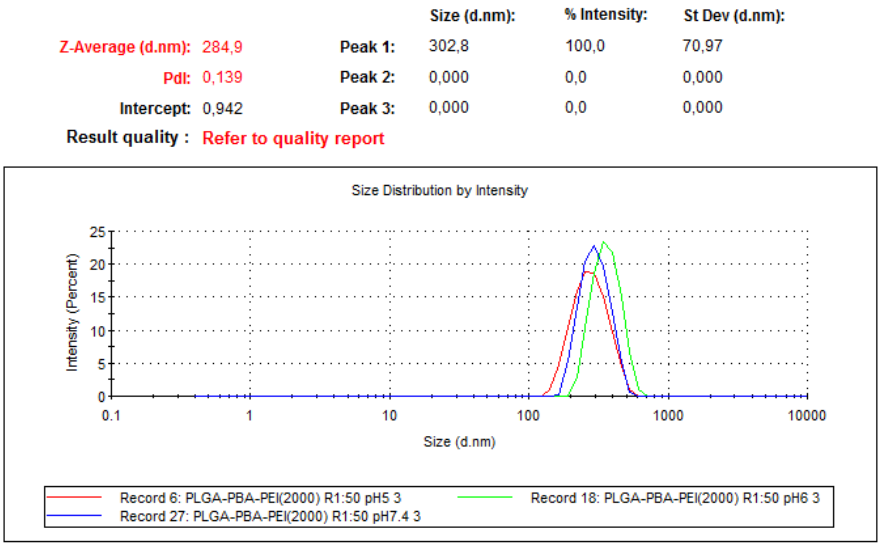

Figure 4.7: *Size for PLGA 1:50 measured with DLS at different pH values. Red line - pH 5. Green line - pH 6. Blue line - pH 7.4. The size of the PLGA 1:50 ranges between 276.6 nm to 320.6 nm.*

These results and size measurements should have been further evaluated and confirmed by complementary methods, such as TEM (Transmission Electron Microscope). TEM measures the dry state of the particles, and the theory of potential contamination could have been determined from these figures. Furthermore, the size of the particles could have been measured from the images. A second synthesis of the particles could also have been performed. This was not done due to not having enough material (mPEG-PBA-PEI_{2000}), and the time to synthesize new material did not fit the project schedule.

The sizes of the PAMAM particles were also confirmed using DLS. In figure 4.8 the intensity and volume PDS from DLS size measurements is presented.

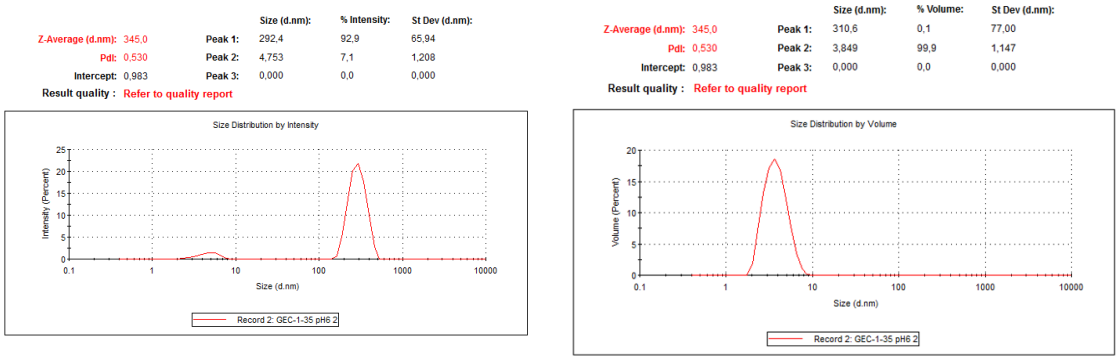

Figure 4.8: *Size of PAMAM-PBA particles measured with DLS at pH 6. Left: Intensity PDS. Right: Volume PDS. The size of the PAMAM particles is around 4.7 nm. The peak at 292.4 nm is most probably aggregated particles.*

To the left (figure 4.8) there was a distinct peak at 292.4 nm, and a smaller peak appeared at 4.7 nm. In the volume PDS (right figure 4.8) a distinct peak was at 3.8 nm. PAMAM-PBA particles are prone to aggregate, which is the most reasonable explanation for the peak at 292.4 nm. In an intensity PDS, the particle's size is determined by the solution's light-scattering properties. Larger nanoparticles will scatter more light than smaller nanoparticles and therefore have a higher intensity than the smaller nanoparticles. A disadvantage of the DLS instrument is that it will measure the light scattering from aggregated particles as one particle. Comparing the intensity PDS to the volume PDS, the potentially aggregated particles' contribution is around 0.1%. Considering this, a conclusion could be drawn that PAMAM-PBA particles had a size around 4.7 nm and that a small percentage of PAMAM-PBA particles had aggregated.

In conclusion, the PLGA 1:10 and PAMAM-PBA nanoparticles demonstrated sizes matching the overall project's goals and aims. The PLGA particles were designed to be around 250 nm and PAMAM around 5 nm. The overall size measurements indicated a successful method for synthesizing the desired nanoparticles.
The results are furthermore promising for reproducible synthesis. Moreover, tuning the size of nanoparticles and modifying the ratio of PBA-PEI polymers can be easily understood. This is, as for the gold nanoparticles (section 2.5), a desired quality for designing nanoparticles.

4.2.2 Charge

The surface charge of the nanoparticles could indicate how they interact with biological systems. Sialic acid, located on glycoproteins on a cell surface are negatively charge. By measuring the particles zeta potential, the electrostatic interactions between the nanoparticles and the glycoproteins could therefore be predicted.

PLGA 1:10 zeta potential varied between 4.56 mV to -2.54 mV for the evaluated pH, seen in figure 4.9. At pH 5, the zeta potential was 4.56 mV. The zeta potential was -0.89 mV at pH 6. For pH 7, the zeta potential was -2.54 mV.

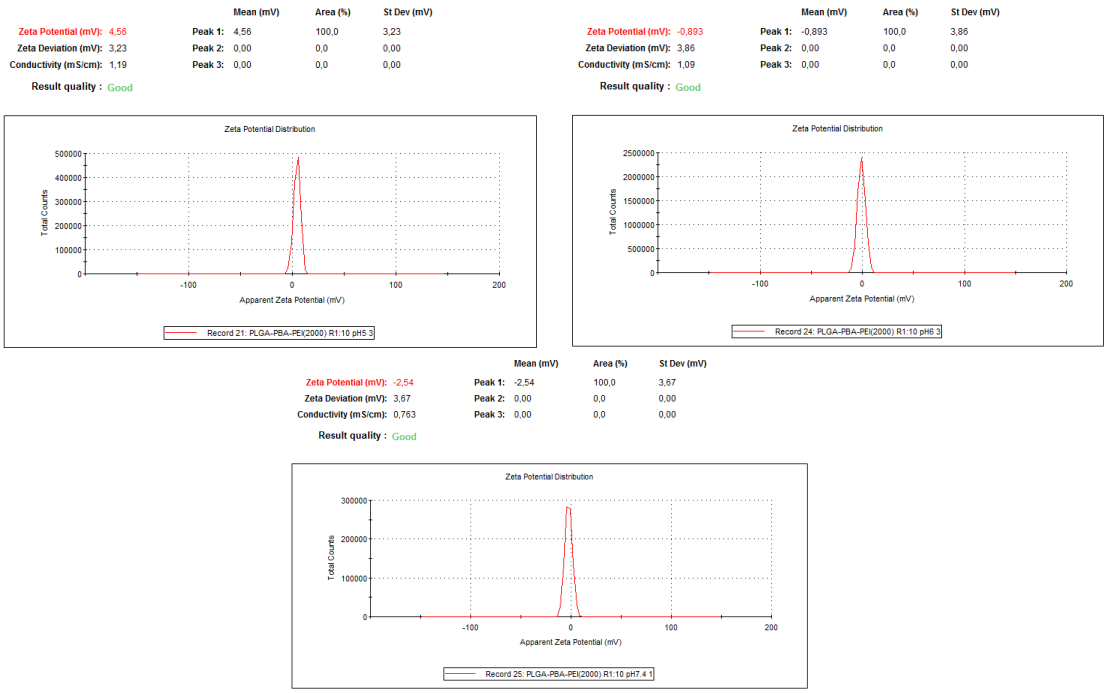

Figure 4.9: *Zeta potential for PLGA 1:10 at different pH values. Top left: pH 5, zeta potential is 4.56 mV. Top right: pH 6, zeta potential is -0.89 mV. Bottom: pH 7.4, zeta potental is -2.54 mV.*

Zeta potential decreased as pH increased, as seen in figure 4.10. The surfactant (PEG) used for PLGA nanoparticles had a slight negative to natural surface charge, and PEI had a strong positive charge, meaning that PBA-PEI_{2000} polymers had a positive charge. As pH increased, the number of hydrogen ions (H^+) decreased, and the number of hydroxide diatomic ion (OH^-) increased. The interactions between the positive H^+ or negative OH^- and the PBA-PEI_{2000} could have lead to conformational changes. These conformational changes could depend on the amino groups being protonated, which would impact binding and cytotoxicity. In addition, these results indicated that the particles might not be stable in the solution as the zeta potential was neither below -30 mV or higher than 30 mV [42]. As the stability was exclusively tested for non-conjugated PLGA particles, it could therefore not be ruled out that the PLGA 1:10 may have been unstable.

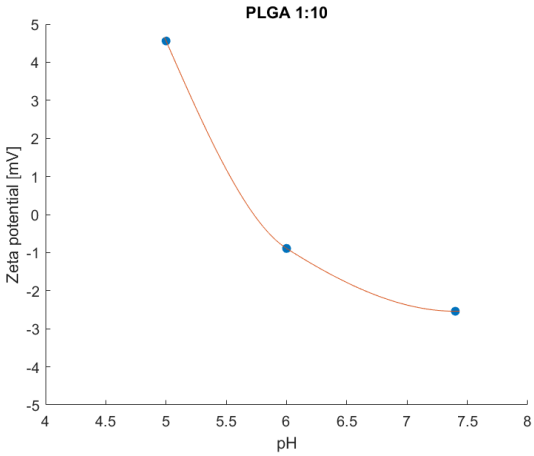

Figure 4.10: *Zeta potential against pH for PLGA 1:10. The trend of the curvature indicates the zeta potential decreases as pH increases.*

The zeta potential for PLGA 1:50 is presented in figure 4.11. At pH 5, the zeta potential was +2.58 mV. For pH 6, the zeta potential was -4.04 mV. At pH 7.4, the zeta potential was -1.57 mV. The results at pH 6 deviated from the findings of PLGA 1:10. The same solution of PLGA 1:50 - pH 6 was used for both the size and zeta potential, and from the same reasoning (size of PLGA 1:50, pH 6) the results may not have been reliable.

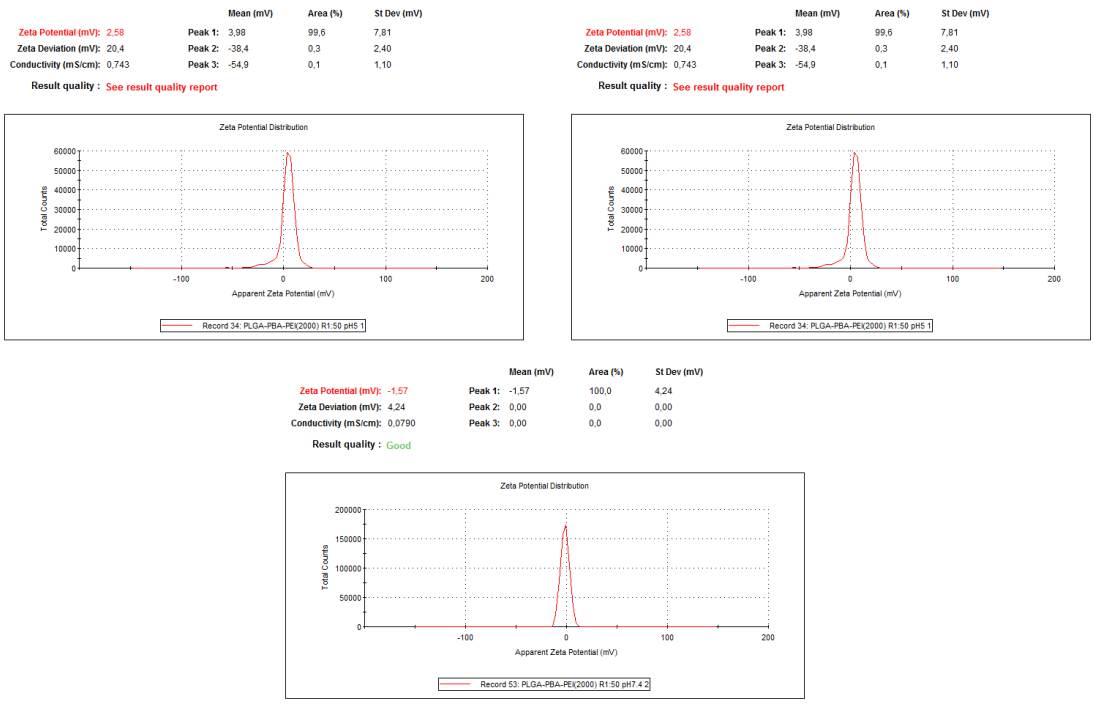

Figure 4.11: *Zeta potential for PLGA 1:50 at different pH values. Top left: pH 5, zeta potential is 2.58 mV. Top right: pH 6, zeta potential is -4.04 mV. Bottom: pH 7.4, zeta potential is -1.57 mV.*

Comparing the zeta potential for PLGA 1:50 at pH 5 and pH 7.4, their zeta potential followed a tendency towards lower zeta potential at increasing pH. Similarly, the size difference between the nanoparticles at pH 5 and pH 7.4 was low. This further confirmed the theory that the PLGA 1:50 at pH 6 could have been contaminated, as previously discussed.
Loose ions in the solution could have interacted with the charges of PBA-PEI_{2000}, resulting in a lower surface charge at pH 6 (figure 4.12). This was not observed for ratio 1:10 of PBA-PEI_{2000} (figure 4.10), meaning that the ratio was the only influence for the different surface charges at pH 6.

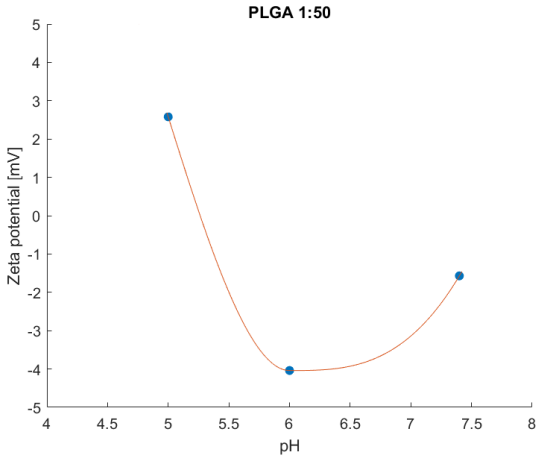

Figure 4.12: *Zeta potential against pH for PLGA 1:50.*

For the PAMAM particles, the zeta potential at pH 6 is shown in figure 4.13. A positive zeta potential, +45.7 mV indicated a higher stability, as literature suggest [42]. The results indicated that the particles could favor binding to negatively charged entities of sialic acid. However, it also indicated the potential of the material being cytotoxic.

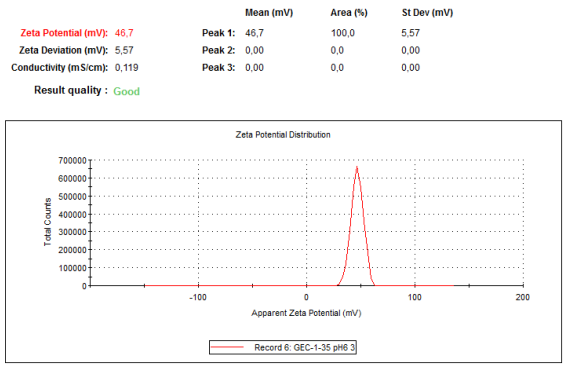

Figure 4.13: *Zeta potential for PAMAM at pH 6. The zeta potential is 45.7 mV which indicates a stable particle.*

In conclusion, both PLGA particles had a negative surface charge at pH 6 and pH 7.4, meaning potential electrostatic repulsion between the PLGA particles and sialic

acid. Positive zeta potential for PAMAM-PBA at pH 6 indicated a potential high binding affinity for sialic acid but possible cytotoxic effect. Therefore, cell studies were preformed to further investigate possible cytotoxicity.

4.3 Cell Studies

A cytotoxicity test was preformed to investigate potential cytotoxicity of the nanoparticles. In a cytotoxicity assay L929 fibroblast cells were used, based on ISO 10993-5 standard. To validate the project's potential for further development it was important to understand the nanoparticles impact on cell death. Nanoparticles resulting in high number of dead cells were not desirable for this project.

This project aimed to stop the cell-to-cell and protein-to-protein signalling. This involved inhibiting cell-to-cell signalling in a leukocyte recruitment process. To confirm the potential for stopping a recruitment process of cells, a migration assay was preformed. For the migration assay, HL60 neutrophils were used as these cells are recruited in the leukocyte recruitment process.

All cell studies were done at physiological pH 7.4.

4.3.1 Cytotoxicity

The nanoparticles PLGA 1:10, PLGA 1:50, and PAMAM were tested for cytotoxicity. From the charge characterization with zeta potential, it was essential to investigate possible cytotoxicity further. Two time points were evaluated, 24 hours and 48 hours. Six different concentrations of particles were added to the cells. P-value was calculated with a one-way ANOVA and compared to the control. A cytotoxic effect is observed if the live cells is below 70%.

As seen in figure 4.14, PLGA 1:10 did not induce any cell death after 24 hours. All treated cells demonstrated a viability above 100 %, compared to the control where cells were only exposed to media. The number of cells increased as the dosage increased (2.5 μg/mL to 100 μg/mL). There was statistical significant difference between the control and dose of particles. The metabolic activity of a cell can increase due to its surroundings. The non-fluorescence dye, resazurin, is reduced by live cell's metabolic activity to a strong fluorescence dye resorufin [43]. The metabolic activity in a cell happens in the mitochondria, where ATP production takes place. The particles added may not have increased the number of live cells but instead increased the cell's metabolic activity. This would mean that a higher number of resazurin molecules were reduced to resorufin molecules. A higher number of fluorescent molecules would yield a higher fluorescent intensity, which would give the impression that there were more cells.
Another reason why it looks like the cells had an increased growth as the dosage increased could be because of cell proliferation. The cells treated with nanoparticles may have been more prone to proliferation than the cells without treatment and increased in number.

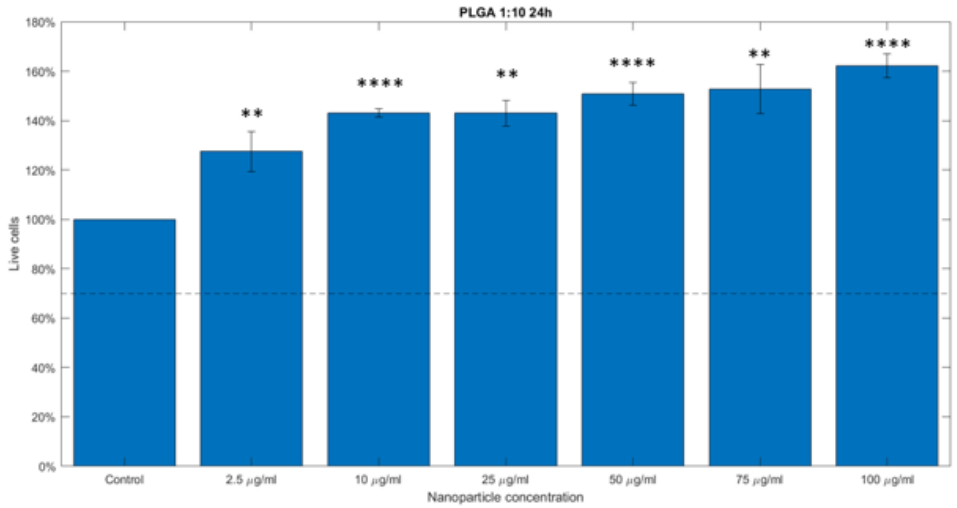

Figure 4.14: *The cytotoxicity for PLGA 1:10 after 24 hours. The control is only live cells, no nanoparticles have been added. The tested concentration of nanoparticles all show an increase in cell viability. The dashed line is at 70 % live cells. Significant test have been done between control and concentration with one way ANOVA: * $P \leq 0.05$, ** $P \leq 0.01$, *** $P \leq 0.001$, **** $P \leq 0.0001$.*

The 48-hour PLGA 1:10 treated cells shown in figure 4.15, indicated a slight decrease in viability compared to the 24-hour plate. All concentrations of the nanoparticle were above the threshold of 70 % live cells. The cell viability ranged from 97 % to 114 % live cells. There was a statistically significant difference between the control and cell treated with 2.5 μg/mL PLGA 1:10. Why there were no statistical difference between the higher doses and control was probably due to the small variance of the 2.5 μg/mL sample.

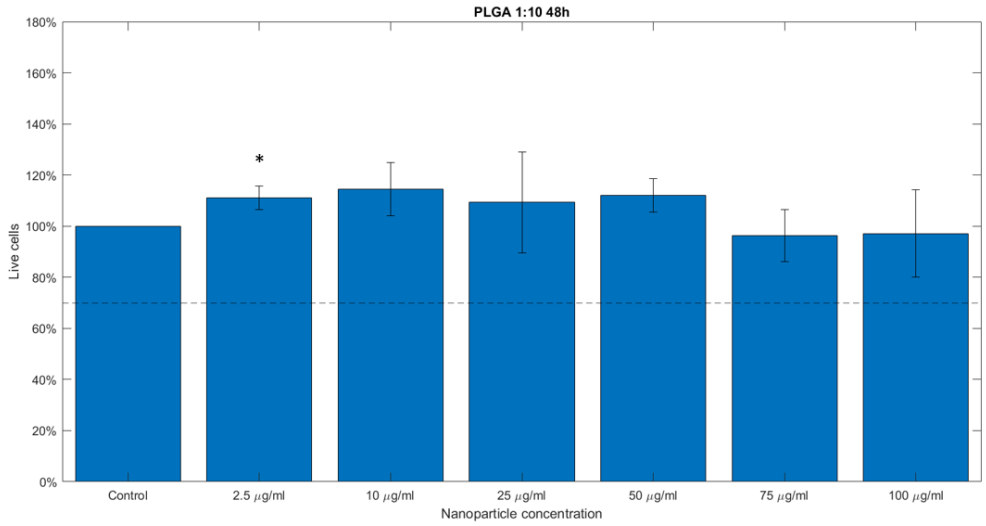

Figure 4.15: *The cytotoxicity for PLGA 1:10 after 48 hours. For the control there is only live cells, no nanoparticles have been added. The tested concentration of nanoparticles shows no cell toxicity. The dashed line is at 70 % live cells. Significant test have been done between control and concentration: * $P \leq 0.05$.*

The difference between 24-hour plate and the 48-hour plate treated with PLGA 1:10 could be due to the number of the resazurin molecules was decreasing. If the 24-hour plate cell count was a result of an increased activity of the cells metabolism due to the resazurin, the number of resazurin molecules would have decrease faster. The fewer number of resazurin molecules could then have lead to a decrease of the metabolic activity of the cells, giving the impression that there was less cells in the 48-hour plate compared to the 24-hour plate. The difference between the 24-hour plate and the 48-hour plate could also be a consequence of pipetting-errors.

As for the PLGA 1:10 particles, PLGA 1:50 had after 24 hours not induced any cell death as seen in figure 4.16. All treated cells had viability over 100 %, compared to the control with only live cells. The dose of the nanoparticles varied from 2.5 μg/mL to 100 μg/mL. Similar to the PLGA 1:10 particles, there was a statistical difference between the control and the different dosages of nanoparticles. For both particles, a high increase in the cell viability was seen after 24 hours, as mentioned above this could be due to either an increase of metabolic activity or cell proliferation.

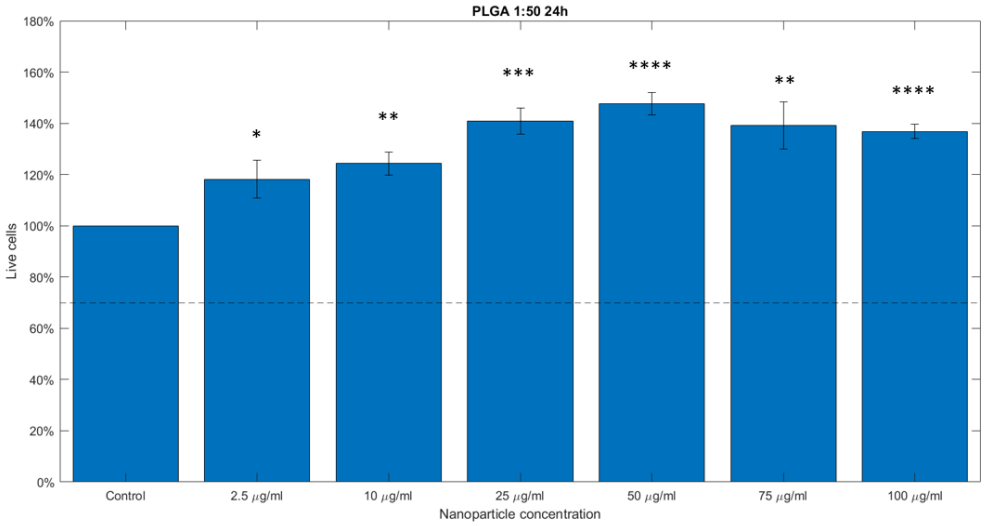

Figure 4.16: *The cytotoxicity for PLGA 1:50 after 24 hours. The control consist of live cells only, no nanoparticles have been added. The tested concentration of nanoparticles all show an increase in cell viability. The dashed line is at 70 % live cells. Significant test have been done between control and concentration with one way ANOVA: * $P \leq 0.05$, ** $P \leq 0.01$, *** $P \leq 0.001$, **** $P \leq 0.0001$.*

The cells that had been treated with PLGA 1:50 for 48 hours are shown in figure 4.17. There was a decrease in cell viability compared to the 24-hour assay. The cell viability ranged from 87 % to 110 % live cells. All concentrations of the nanoparticle were over the threshold of 70 % live cells. Cells treated with 25 μg/mL had viability under 100 %, but there where no significant difference between 25 μg/mL and control. For the concentration of 10 μg/mL, there was a significant difference compared to the control on a 0.05 level. The possible reasons behind the increased number of alive cells have been discussed above.

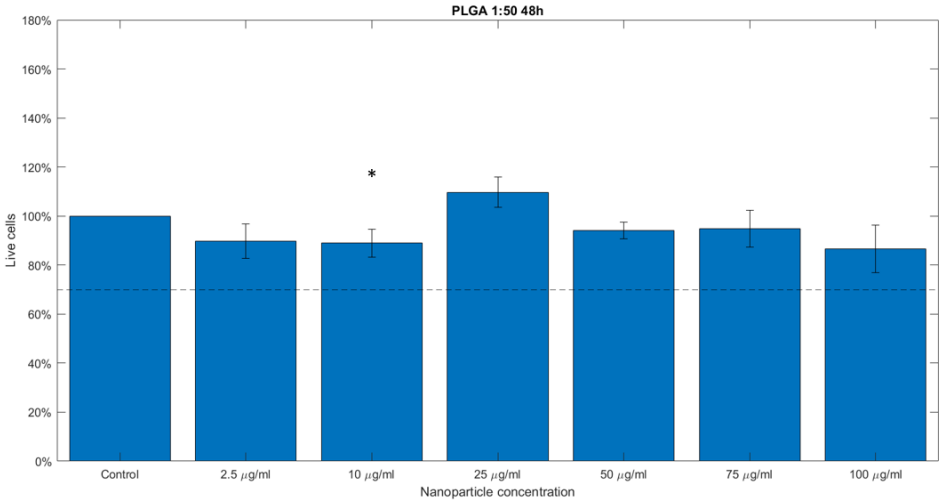

Figure 4.17: *The cytotoxicity for PLGA 1:50 after 48 hours. For the control there is only live cells, no nanoparticles have been added. The tested concentration of nanoparticles shows no cell toxicity. The dashed line is at 70 % live cells. Significant test have been done between control and concentration with one way ANOVA: * $P \leq 0.05$*

The cell viability results for the PAMAM are shown in figure 4.18. The cell viability after 24 hours ranged from 82 % to 96 %. All concentrations of the nanoparticle were over the threshold of 70 % live cells. The different PAMAM nanoparticle concentrations showed a significant difference to the control except for cells treated with 75 μg/mL concentration.

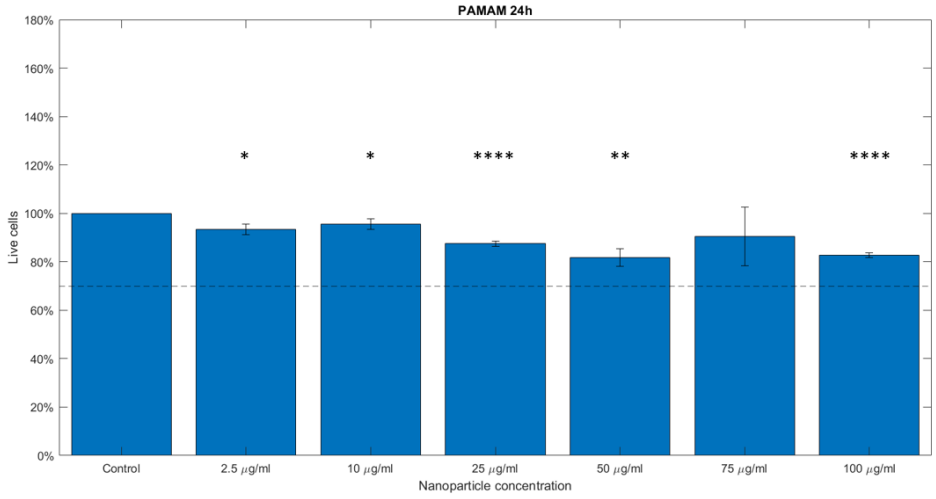

Figure 4.18: *The cytotoxicity for PAMAM after 24 hours. For the control there is only live cells, no nanoparticles have been added. The tested concentration of nanoparticles shows no cell toxicity. The dashed line is at 70 % live cells. Significant test have been done between control and concentration with one way ANOVA: * $P \leq 0.05$, ** $P \leq 0.01$, *** $P \leq 0.001$, **** $P \leq 0.0001$.*

PAMAM had, after 48 hours, not induced any cell death as seen in figure 4.19. All treated cells showed no cytotoxicity. This result was not expected as the zeta potential for PAMAM-PBA was high (figure 4.13). Surface charge was not the only factor for potential cell toxicity; the particles' dose, size, and shape could also influence. The percentage of alive cells varied from 82 % to 110 %. There was a statistically significant difference between the control and the different concentrations of PAMAM except for the 10 μg/mL to 50 μg/mL concentrations.

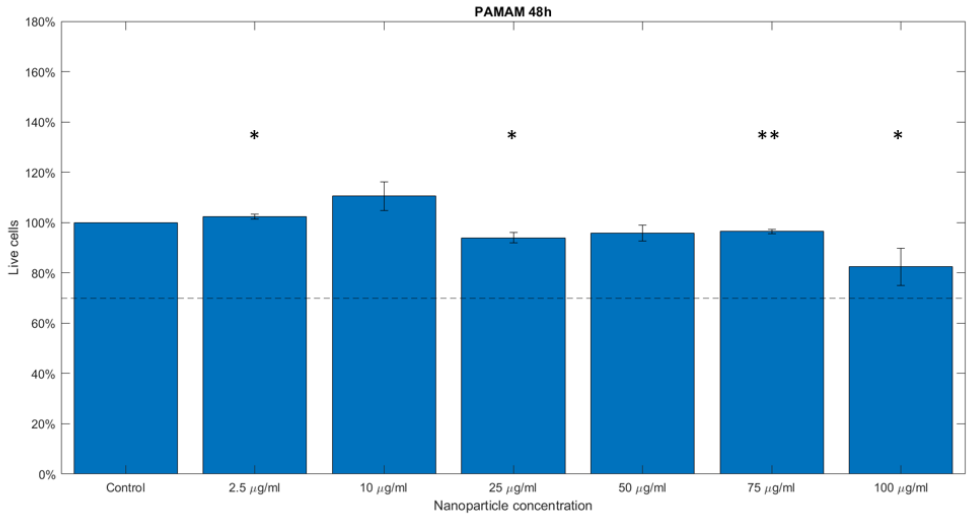

Figure 4.19: *The cytotoxicity for PAMAM after 48 hours. For the control there is only live cells, no nanoparticles have been added. The tested concentration of nanoparticles shows no cell toxicity. The dashed line is at 70 % live cells. Significant test have been done between control and concentration with one way ANOVA: * $P \leq 0.05$, ** $P \leq 0.01$.*

The PAMAM-PBA had induced more cell death than the PLGA nanoparticles. The results from the zeta potential (figure 4.13, 4.9 and 4.11) showed a high positive surface charge for PAMAM and the PLGA nanoparticles showed a negative surface charge at pH 7.4. PAMAM-PBA were believed to be cytotoxic, but the dosages tested proved not to be. This indicated that the tested concentrations of the nanoparticles would be safe to use for further cell studies and applications.

4.3.2 Migration Assay

To evaluate if the nanoparticles could inhibit leukocyte recruitment, a preliminary migration assay with neutrophils (HL60) was performed (figure 4.20. Neutrophil migration was assayed towards the bacteria cell wall component lipopolysaccharide, LPS. While it is known that LPS can activate these cells, it was not an optimal migration attractant. Due to unforeseen circumstances this component had to be used instead of a stronger and more specific migration attractant. The assay was only performed once, and conclusions that could drawn were limited.

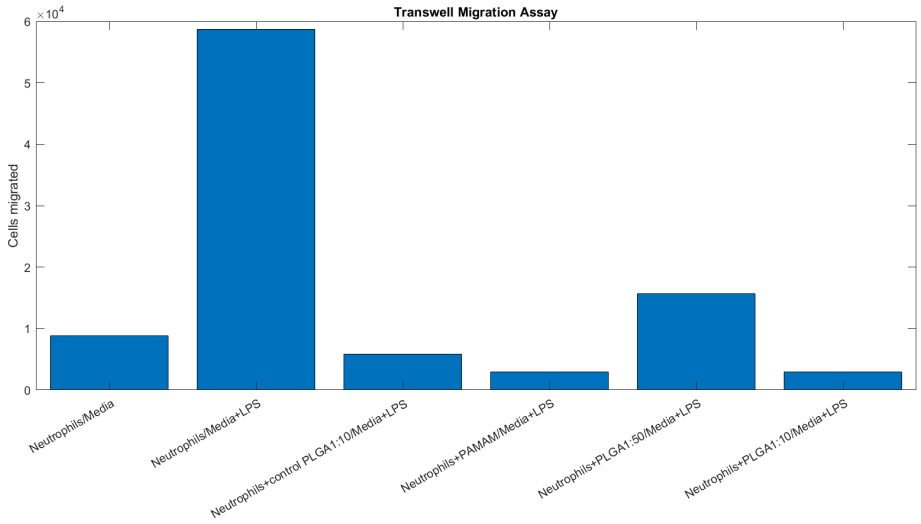

Figure 4.20: *Transwell migration assay. Number of cells migrated left to right: 8800, 58650, 5850, 2930, 14650, 2930.*

The migration assay preformed would indicate if the nanoparticles could inhibit the migration of HL60 cells. In total there were 500 000 cells that could potentially have migrate towards the lower well (see figure 3.1). The wells treated with PLGA 1:10, PLGA 1:50 and, PAMAM particles should have had a high cell count in the top wells, and a low cell count in the lower wells treated with LPS.
After 4 hours, the neutrophils had not migrated towards media to the same extent as they had to the media containing LPS. All the wells treated with particles reduced migration compared to the positive control containing LPS only. Cells treated with PLGA 1:10 migrated less than both untreated neutrophils migrating towards LPS and treated neutrophils migrating towards media control. A higher number of cells were found in the lower wells after PLGA 1:50 treatment as compared to media. More interesting was that the PLGA 1:10 control particle seemed to inhibit migration better than neutrophils treated with PLGA 1:50. This could be due to the PEI conjugated on the control particle. It was not expected to inhibit neutrophils efficiently without the PBA conjugated onto the PEI.

LPS used to stimulate the migration of cells was not optimal. LPS has been reported to activate neutrophils [44], not migrate towards it. Furthermore, the PLGA nanoparticles was to inhibit leukocyte recruitment from the vascular endothelial layer to the tissue. The endothelial layer of cells was not added between the top and bottom well. Many improvements could have be made for the migration assay, and the results need to be validated.

The low number of cells recovered after the migrations assay indicated that the results may not be reliable. The migration assay started with 500 000 cells per well. When measuring both migrated cells and cells that had not migrated (located in the top well, see figure 3.1), the total number of cells was well below 500 000. Furthermore, the number of total cells in each well varied from 26 380 to 117 300. At best, about 1/5 of the cells were counted. A high variation in the cells counted

made the result less reliable. The experiment should have been run in triplicates to get a more reliable result. However, due to time restrictions, this was not done.

In theory, the particles could inhibit a leukocyte recruitment but could not be demonstrated due to the limitations of the assay. In summary, the PAMAM particles and the PLGA 1:10 showed potential of inhibiting migration of neutrophils. The PLGA 1:50 did not show promising results for inhibiting migration. Interestingly, the control PLGA 1:10, conjugated with only PEI, also showed potential of inhibiting migration of neutrophils.

Inhibiting leukocyte recruitment would remove the need for anti-inflammatory drugs that can cause unwanted and serious side effects (section 2.5).

5
Conclusion

This project aimed to inhibit inflammation. To succeed with this, nanoparticles were synthesized and conjugated with PBA-PEI. It was hypothesized that PBA-PEI had a high specificity and binding affinity towards sialic acid, a highly upregulated monosaccharide during an inflammation. Using nanoparticles conjugated with PEI, inflammation could be inhibited by preventing cell-to-cell signaling and protein-to-protein signaling. The results showed that PBA had a specificity to monosaccharides by UV studies. PBA-PEI had both specificity and a high binding affinity to sialic acid over other monosaccharides, as demonstrated by ITC measurements. Furthermore, we developed a method for synthesizing PLGA and PAMAM nanoparticles conjugated with PBA-PEI. The nanoparticles showed no cytotoxicity for the tested concentrations after 24 and 48 hours. Moreover, the migration assay did not succeed for various reasons. The potential for the nanoparticles to inhibit the migration of leukocytes was, however, positive.

In conclusion, the PBA-PEI polymer has a high potential for inhibiting cell-to-cell or protein-to-protein contacts when conjugated to a nanoparticle. The conclusion comes from the PBA-PEI polymer's high binding affinity and specificity to sialic acid in inflammatory pH. Furthermore, the conjugated nanoparticles were biocompatible and would not harm cells at tested concentrations.

6
Future Research

The PBA-PEI polymer has excellent potential for inhibiting immune responses. The next step would be to evaluate the nanoparticle's binding affinity to sialic acid using ITC. To see the possible inhibition of leukocyte recruitment an improved migration assay should be designed.
As the PBA-PEI have a high binding affinity and selectivity to sialic acid one could look at Sialyl-Lewis X (sLe^X). Sialic acid is part of the sLe^X which is a fucosylated and sialylated tetrasaccharide, shown in figure 6.1.

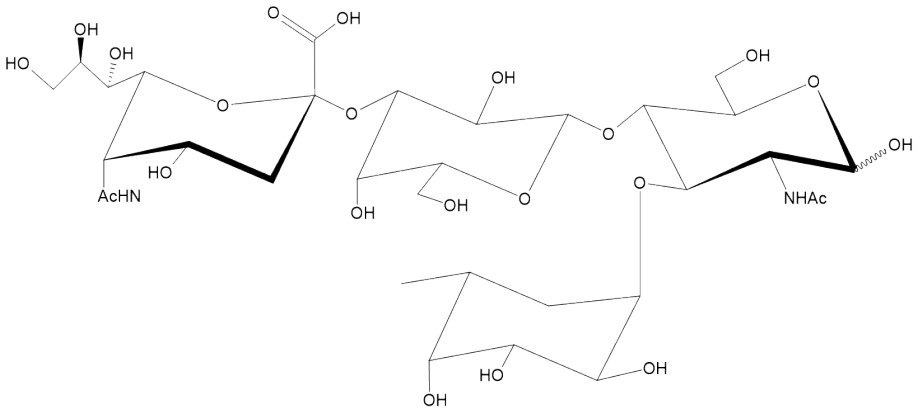

Figure 6.1: *Molecular structure of Sialyl-Lewis X.*

SLe^X decorates glycans and is one of the best ligands for selectins. All selectins can bind to sLe^X with high affinity but, sLe^X is not the only determinant for selectin binding. Nontheless, it is still important to remember that sLe^X do have a crucial role for the selectin binding [3]. The binding between PBA-PEI_{2000} conjugated PLGA nanoparticles and SLe^X has the potential to stop leukocyte recruitment and could be measures in ITC.

Apart from inflammation cells, cancer cells also have upregulated sialic acid. For potential tumor imaging a dye could be conjugated to the nanoparticle [45]. This could mean earlier detection of cancer cells, evaluation of therapeutic responses, or similar applications. In the case of surgically removing a tumor, a higher quality image can help the surgeon avoid leaving cancer cells behind or removing healthy tissue. The field of saccharide-targeting medicine is rapidly expanding yet needs novel tools to develop further, and significant progress has been made with nanomedicine as a significant contributor.

Bibliography

[1] J. 'Mölne and A. 'Wold, *Inflammation*. Liber, 1 ed., 1 2007.

[2] H. B. Fleit, "Chronic Inflammation," in *Pathobiology of Human Disease: A Dynamic Encyclopedia of Disease Mechanisms*, pp. 300–314, Elsevier Inc., 1 2014.

[3] B. A. Smith and C. R. Bertozzi, "The clinical impact of glycobiology: targeting selectins, Siglecs and mammalian glycans," 1 2021.

[4] "Chemical Glycobiology: Study of Glycans and the Immune System."

[5] B. A. Cobb and D. L. Kasper, "Coming of age: Carbohydrates and immunity," *European Journal of Immunology*, vol. 35, pp. 352–356, 2 2005.

[6] F. Erra Díaz, E. Dantas, and J. Geffner, "Unravelling the interplay between extracellular acidosis and immune cells," 2018.

[7] V. Ajit, M. E. Etzler, R. D. Cummings, and J. D. Esko, "Chapter 26 Discovery and Classification of Glycan-Binding Proteins TWO MAJOR CLASSES OF GLYCAN-BINDING PROTEINS — LECTINS AND," pp. 1–10, 2009.

[8] E. Maverakis, K. Kim, M. Shimoda, M. E. Gershwin, F. Patel, R. Wilken, S. Raychaudhuri, L. R. Ruhaak, and C. B. Lebrilla, "Glycans in the immune system and The Altered Glycan Theory of Autoimmunity: A critical review," 2 2015.

[9] C. Traving and R. Schauer, "Review Structure, function and metabolism of sialic acids," tech. rep., 1998.

[10] A. Varki, "Sialic acids in human health and disease," 8 2008.

[11] K. F. Bornhöfft, T. Goldammer, A. Rebl, and S. P. Galuska, "Siglecs: A journey through the evolution of sialic acid-binding immunoglobulin-type lectins," 9 2018.

[12] A. Varki, R. L. Schnaar, and R. Schauer, *Sialic Acids and Other Nonulosonic Acids*. Cold Spring Harbor Laboratory Press, 2015.

[13] J. M. Berg, J. L. Tymoczko, and L. Stryer, "Lectins Are Specific Carbohydrate-Binding Proteins," 2002.

[14] B. Lepenies, T. Johannssen, J. Hütter, and S. Zimmermann, "C-type lectins," in *Glycoscience: Biology and Medicine*, pp. 675–683, Springer Japan, 1 2015.

[15] K. Ley, "The role of selectins in inflammation and disease," 6 2003.

[16] W. A. Muller, "Getting Leukocytes to the Site of Inflammation,"

[17] M. Leick, V. Azcutia, G. Newton, and F. W. Luscinskas, "Leukocyte recruitment in inflammation: Basic concepts and new mechanistic insights based on new models and microscopic imaging technologies," 2014.

[18] M. Sperandio, C. A. Gleissner, and K. Ley, "Glycosylation in immune cell trafficking,"

[19] J. Yan, G. Springsteen, S. Deeter, and B. Wang, "The relationship among pK a, pH, and binding constants in the interactions between boronic acids and diols - It is not as simple as it appears," *Tetrahedron*, vol. 60, pp. 11205–11209, 11 2004.

[20] A. Stubelius, S. Lee, and A. Almutairi, "The Chemistry of Boronic Acids in Nanomaterials for Drug Delivery," *Accounts of Chemical Research*, vol. 52, pp. 3108–3119, 11 2019.

[21] A. Di Pasquale, S. Tommasone, L. Xu, J. Ma, and P. M. Mendes, "Cooperative Multipoint Recognition of Sialic Acid by Benzoboroxole-Based Receptors Bearing Cationic Hydrogen-Bond Donors," *Journal of Organic Chemistry*, vol. 85, pp. 8330–8338, 7 2020.

[22] H. Otsuka, E. Uchimura, H. Koshino, T. Okano, and K. Kataoka, "Anomalous Binding Profile of Phenylboronic Acid with N-Acetylneuraminic Acid (Neu5Ac) in Aqueous Solution with Varying pH," 2003.

[23] M. Ji, P. Li, N. Sheng, L. Liu, H. Pan, C. Wang, L. Cai, and Y. Ma, "Sialic Acid-Targeted Nanovectors with Phenylboronic Acid-Grafted Polyethylenimine Robustly Enhance siRNA-Based Cancer Therapy," 2016.

[24] S. Deshayes, H. Cabral, T. Ishii, Y. Miura, S. Kobayashi, T. Yamashita, A. Matsumoto, Y. Miyahara, N. Nishiyama, and K. Kataoka, "Phenylboronic Acid-Installed Polymeric Micelles for Targeting Sialylated Epitopes in Solid Tumors," 2013.

[25] "pKa Definition in Chemistry."

[26] Q. Peng, F. Chen, Z. Zhong, and R. Zhuo, "Enhanced gene transfection capability of polyethylenimine by incorporating boronic acid groupsw,"

[27] P. K. Maiti, T. Çağin, S. T. Lin, and W. A. Goddard, "Effect of solvent and pH on the structure of PAMAM dendrimers," *Macromolecules*, vol. 38, pp. 979–991, 2 2005.

[28] Y. Cui, B. Liang, L. Wang, L. Zhu, J. Kang, H. Sun, and S. Chen, "Enhanced biocompatibility of PAMAM dendrimers benefiting from tuning their surface charges," *Materials Science and Engineering C*, vol. 93, pp. 332–340, 12 2018.

[29] E. M. Elmowafy, M. Tiboni, and M. E. Soliman, "Biocompatibility, biodegradation and biomedical applications of poly(lactic acid)/poly(lactic-co-glycolic acid) micro and nanoparticles," vol. 49, pp. 347–380, 2019.

[30] F. Danhier, E. Ansorena, J. M. Silva, R. Coco, A. Le Breton, and V. Préat, "PLGA-based nanoparticles: An overview of biomedical applications," 7 2012.

[31] S. A. Malik, W. H. Ng, J. Bowen, J. Tang, A. Gomez, A. J. Kenyon, and R. M. Day, "Electrospray synthesis and properties of hierarchically structured PLGA TIPS microspheres for use as controlled release technologies," *Journal of Colloid and Interface Science*, vol. 467, pp. 220–229, 4 2016.

[32] W. Huang and C. Zhang, "Tuning the Size of Poly(lactic-co-glycolic Acid) (PLGA) Nanoparticles Fabricated by Nanoprecipitation," *Biotechnology Journal*, vol. 13, 1 2018.

[33] C. J. Martínez Rivas, M. Tarhini, W. Badri, K. Miladi, H. Greige-Gerges, Q. A. Nazari, S. A. Galindo Rodríguez, R. Román, H. Fessi, and A. Elaissari, "Nanoprecipitation process: From encapsulation to drug delivery," 10 2017.

[34] N. M. Gulati, P. L. Stewart, and N. F. Steinmetz, "Bioinspired Shielding Strategies for Nanoparticle Drug Delivery Applications," 8 2018.
[35] M. E. Ali and A. Lamprecht, "Polyethylene glycol as an alternative polymer solvent for nanoparticle preparation.," *International journal of pharmaceutics*, vol. 456, pp. 135–142, 11 2013.
[36] A. Aderem and K. D. Smith, "A systems approach to dissecting immunity and inflammation," *Seminars in Immunology*, vol. 16, pp. 55–67, 2 2004.
[37] C. I. Wyatt Shields, L. Li-Wen Wang, M. A. Evans, S. Mitragotri, and J. A. Paulson, "Materials for Immunotherapy,"
[38] K. E. Wellen and G. S. Hotamisligil, "Inflammation, stress, and diabetes," *Journal of Clinical Investigation*, vol. 115, pp. 1111–1119, 5 2005.
[39] R. Chovatiya and R. Medzhitov, "Stress, inflammation, and defense of homeostasis," 4 2014.
[40] "D-Fructose | C6H12O6 - PubChem."
[41] B. Wang and J. Brand-Miller, "The role and potential of sialic acid in human nutrition," 11 2003.
[42] M. Instruments, "Tech Note: Zeta potential - An introduction in 30 minutes," tech. rep.
[43] J. S. Uzarski, M. D. DiVito, J. A. Wertheim, and W. M. Miller, "Essential design considerations for the resazurin reduction assay to noninvasively quantify cell expansion within perfused extracellular matrix scaffolds," *Biomaterials*, vol. 129, pp. 163–175, 6 2017.
[44] N. E. Gomes, M. K. Brunialti, M. E. Mendes, M. Freudenberg, C. Galanos, and R. Salomão, "Lipopolysaccharide-induced expression of cell surface receptors and cell activation of neutrophils and monocytes in whole human blood," *Brazilian Journal of Medical and Biological Research*, vol. 43, pp. 853–859, 9 2010.
[45] S. V. Glavey, D. Huynh, M. R. Reagan, S. Manier, M. Moschetta, Y. Kawano, A. M. Roccaro, I. M. Ghobrial, L. Joshi, and M. E. O'Dwyer, "The cancer glycome: Carbohydrates as mediators of metastasis," *Blood Reviews*, vol. 29, no. 4, pp. 269–279, 2015.

A

Appendix 1

A.1 Method development of PLGA nanoparticles

The PLGA nanoparticles was based on literature [32]. DLS was used to characterize the size of the nanoparticles. For surfactant different (w/v) % of PEG in milli-Q or Pluronic F-127 was evaluated:

- 0.1% PEG in milli-Q
- 0.5% PEG in milli-Q
- 1.0% PEG in milli-Q/Pluronic F-127
- 2.0% PEG in milli-Q

PLGA was dissolved in acetone or chloroform in following concentrations:

- 40 mg/ml PLGA in acetone
- 25 mg/ml PLGA in acetone
- 20 mg/ml PLGA in acetone/cloroform
- 17 mg/ml PLGA in acetone
- 15 mg/ml PLGA in acetone

The PLGA solution was added drop wise in PEG solution under stirring in room temperature with a 21G needle.

The most successful for 200 nm is presented in figure A.1

		Size (d.nm):	% Intensity:	St Dev (d.nm):
Z-Average (d.nm): 195,7	Peak 1:	213,0	100,0	63,93
PdI: 0,064	Peak 2:	0,000	0,0	0,000
Intercept: 0,973	Peak 3:	0,000	0,0	0,000
Result quality : Good				

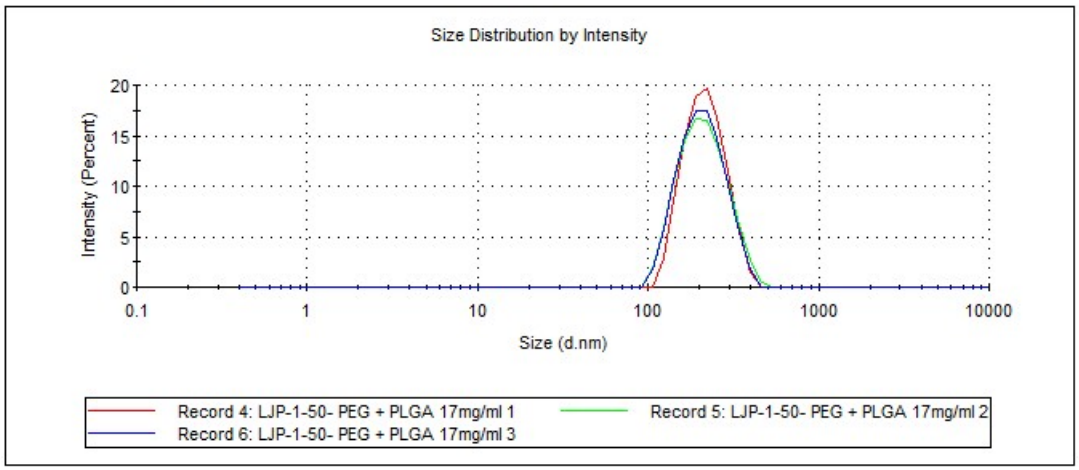

Figure A.1: *DLS data for PLGA particles with a size around 200 nm. 1% PEG solution in milli-Q water with 17mg/ml PEG solution in acetone.*

B

Appendix 2

All of the methods, results and figures in Appendix 2 belongs to Gizem Erensoy.

B.1 NMR data

B.1.1 3-CPBA

Hydrogen NRM:

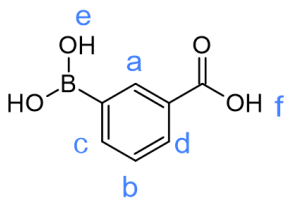

Figure B.1: *3-CPBA with hydrogen atoms labeled.*

H-NMR (figure B.2), (400 MHz), (DMSO-d6), ppm: 2.48 (dt, DMSO-d6 peak); 7.44 (t, 1H, Hb); 7.84-8.35 (m, 4H, Hc, Hd, He); 8.40 (s, 1H, Ha); 12.92 (s, 1H, Hf).

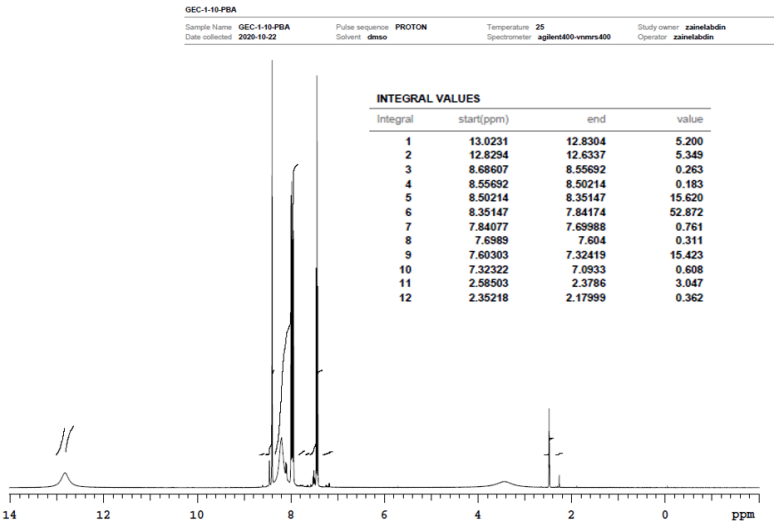

Figure B.2: *H-NMR data for 3-CPBA*

Carbon NRM:

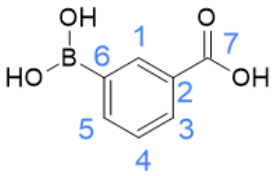

Figure B.3: *3-CPBA with carbon atoms labeled.*

C-NMR (figure B.4, (400 MHz), (DMSO-d6), ppm: 40 (DMSO-d6 peak); 128.06(C4); 130.25 (C2); 131.32 (C3); 135.59 (C1); 138.88 (C5); 168.13 (C7).

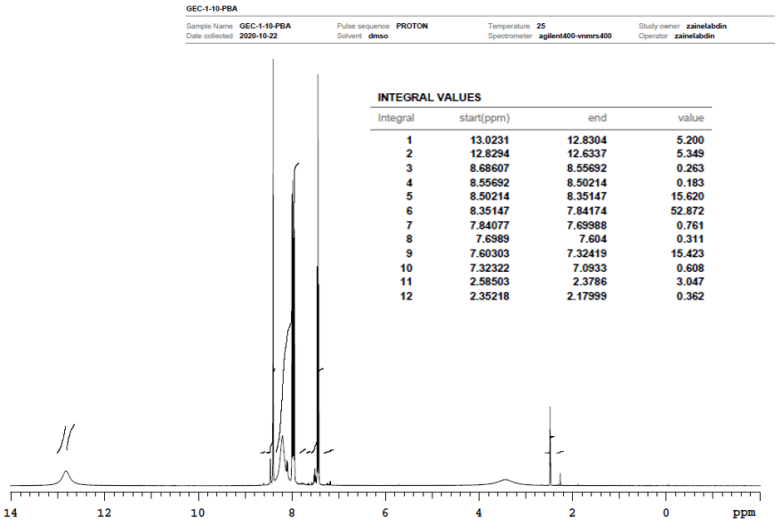

Figure B.4: *C-NMR data for 3-CPBA*

B.1.2 PBA-PEI$_{2000}$

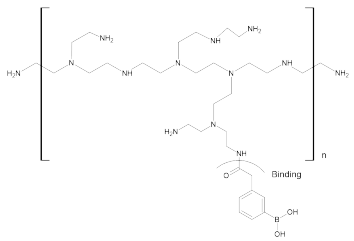

Figure B.5: *PBA-PEI*

H-NMR (figure B.7), (400 MHz), (DMSO-d6), ppm: 2.34-3.03 (-CH2-CH2-NH2 protons of PEI); 7.40-8.11 (m, 12H, aromatic protons on PBA)

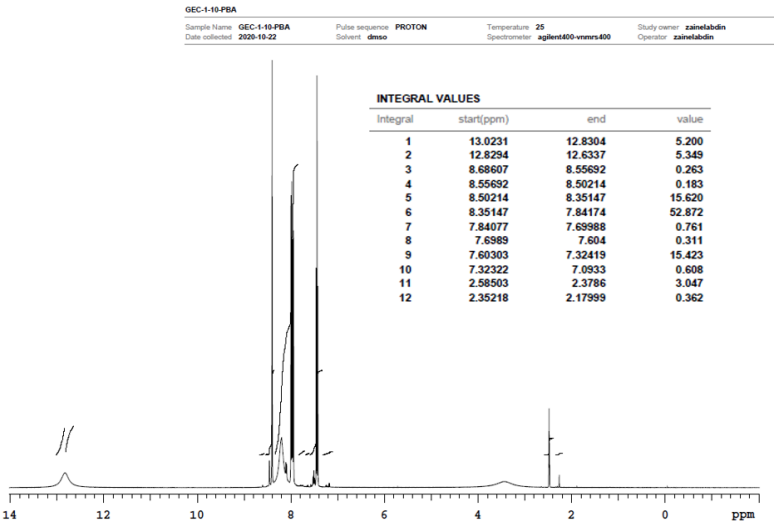

Figure B.6: *H-NMR data for PBA-PEI*$_{2000}$

B.2 PAMAM synthesis

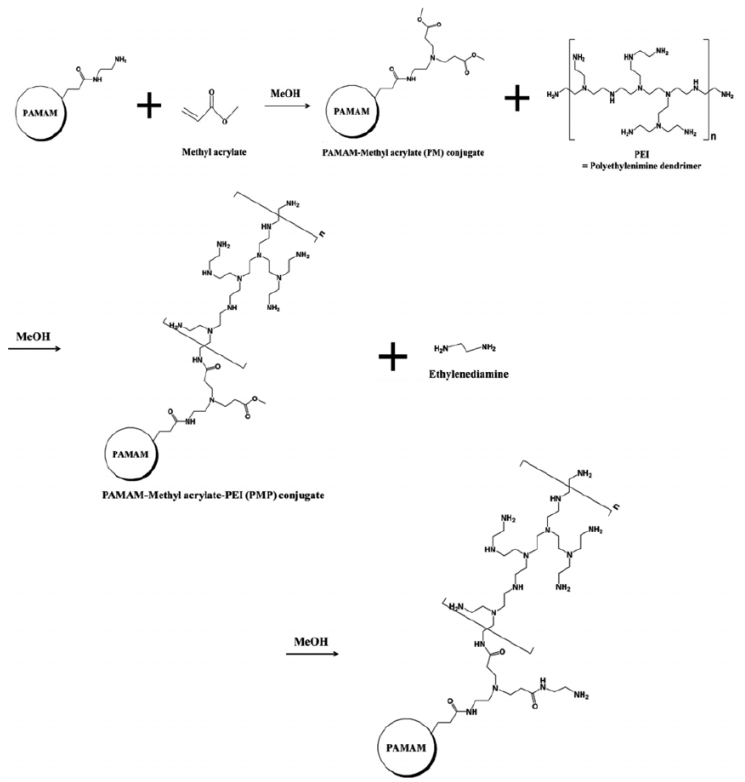

Figure B.7: *Conjugation scheme for PAMAM nanoparticles.*

Remove original PAMAM solvent (methanol) using nitrogen gas. Half of the original stock will be used. Re-dissolve PAMAMs in pure water and lyophilize overnight. PAMAM G5 was dissolved in methanol. (Number of surface groups x 200) fold molar

ratio of methyl acrylate (MA) was added to solution. Solution was stirred under nitrogen atmosphere for 3 days, 40 °C. Solvent was evaporated under vacuum and quenched by the addition of excess amount of cold diethyl ether. Precipitated sample (PAMAM-MA) dissolved in methanol with 1-fold molar ratio of PEI derivative. The solution was stirred in a nitrogen atmosphere at 40 °C for 2 days. 1 mL of ethylenediamine was added and the solution was stirred in a nitrogen atmosphere at 40 °C for 1 day, and the sample was quenched by the addition of an excess amount of cold ethyl ether. The precipitated product was solubilized in water and dialyzed for 1 day against distilled water using dialysis membrane (MWCO 3,500). The final product freeze dried.